

**UNCLASSIFIED**

**AD 408 926**

**DEFENSE DOCUMENTATION CENTER**

**FOR**

**SCIENTIFIC AND TECHNICAL INFORMATION**

**CAMERON STATION, ALEXANDRIA, VIRGINIA**



**UNCLASSIFIED**

**NOTICE:** When government or other drawings, specifications or other data are used for any purpose other than in connection with a definitely related government procurement operation, the U. S. Government thereby incurs no responsibility, nor any obligation whatsoever; and the fact that the Government may have formulated, furnished, or in any way supplied the said drawings, specifications, or other data is not to be regarded by implication or otherwise as in any manner licensing the holder or any other person or corporation, or conveying any rights or permission to manufacture, use or sell any patented invention that may in any way be related thereto.

THE PENNSYLVANIA STATE UNIVERSITY  
Department of Mechanical Engineering

INVESTIGATIONS ON THE  
INTAKE INDUCED AIR SWIRL  
OF A STRATIFIED CHARGE ENGINE

Theoretical and Experimental Investigations

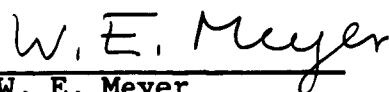
May 1963

Technical Report No. 1  
Experimental Development of a  
Novel Stratified Charge Engine  
Contract No.  
DA-36-034-ORD-3638-T  
U. S. Army Materiel Command  
Army Tank-Automotive Center  
Detroit Arsenal

Prepared by:

  
Robert A. Taylor  
Research Assistant in  
Mechanical Engineering

Approved by:

  
W. E. Meyer  
Professor of  
Mechanical Engineering

## ABSTRACT

Various methods of generating air swirl in a four-stroke-cycle piston engine cylinder were investigated on a flow model constructed to simulate the engine intake process under steady flow conditions. The investigation was centered on the production and control of the swirl for a spark-ignited stratified charge engine in which stratification is produced by the interaction of the injected fuel spray with the swirling air in the cylinder.

Flow mapping and observations were conducted in the model with paddle wheels, tufted grid, and a hot-wire anemometer. Turbulent intensities were mapped and transient flows were studied also, using hot-wire techniques.

The model flow results were analyzed using basic equations of viscous fluids. This information was then extended to postulate the character of the actual flow in the engine cylinder during compression.

The results indicated that the best swirl generation method is one that produces a swirl upstream of the intake valve, but in the direction of the cylinder axis. The means for accomplishing this show good possibilities for varying swirl rate in accordance with engine requirements.

ACKNOWLEDGEMENTS

The author wishes to express his appreciation to Dr. A. W. Hussmann, Professor of Mechanical Engineering, for his encouraging assistance during the initial phases of the investigation; to W. E. Meyer, Professor of Mechanical Engineering, for his guidance and helpful suggestions during the remainder of the investigation; and to Dr. D. P. Margolis and Dr. M. Poreh for their instruction in turbulence mapping and probe making techniques.

Appreciation is also extended to Mr. William M. Glass and the members of the Technical Services staff; and to the student helpers, particularly to J. C. Miller and K. L. Gardner for their assistance in the experimental program.

The work reported here was done in the Department of Mechanical Engineering, The Pennsylvania State University, and was sponsored by the Army Tank-Automotive Center, Detroit Arsenal, under Contract No. DA-36-034-ORD-3638-T.

TABLE OF CONTENTS

	Page
Acknowledgements . . . . .	ii
List of Figures . . . . .	v
Nomenclature . . . . .	viii
I. INTRODUCTION . . . . .	1
1.1 General Statement of the Problem . . . . .	1
1.2 Origin and Importance of the Study . . . . .	3
1.3 Previous Related Studies . . . . .	5
Engine Studies . . . . .	6
Steady Flow Model Studies . . . . .	8
1.4 Specific Statement of the Problem . . . . .	9
Hypothesis to be Investigated . . . . .	9
Air Swirl Control . . . . .	10
Turbulence . . . . .	10
1.5 Scope and Limitation of the Study . . . . .	11
II. PROCEDURE OF THE INVESTIGATION . . . . .	13
2.1 Model Design . . . . .	13
2.2 Experimental Apparatus . . . . .	13
2.3 Flow Investigations . . . . .	21
Qualitative Observations . . . . .	21
Flow Mapping . . . . .	21
Calibration . . . . .	23
Azimuth Measurements . . . . .	23
Radial Velocity Measurements . . . . .	27
2.4 Turbulence Investigations . . . . .	27
2.5 Transient Flow Studies . . . . .	28
2.6 Swirl Generators . . . . .	28
III. EXPERIMENTAL RESULTS . . . . .	34
3.1 Geometric Investigations . . . . .	34
3.2 Air Swirl Rate Control . . . . .	36
External Method . . . . .	41
3.3 Time-Distance Relationship Studies . . . . .	43
Swirl Development . . . . .	46
Transient Mapping . . . . .	48
3.4 Air Swirl Symmetry . . . . .	48
3.5 Turbulence Measurements . . . . .	55
IV. ANALYSIS OF RESULTS AND HYPOTHESIS . . . . .	61
4.1 Analysis of Results . . . . .	61
Effect of Viscosity . . . . .	62
4.2 Analysis of the Hypothesis . . . . .	64
4.3 Engine Considerations . . . . .	65
Compression of Vorticity . . . . .	70
4.4 Efficiency Considerations . . . . .	73

	Page
V. SUMMARY AND CONCLUSIONS	77
5.1 Statement of the Problem. . . . .	77
5.2 Origin and Importance of the Problem. . .	77
5.3 Procedure . . . . .	78
5.4 Results and Conclusions . . . . .	79
5.5 Suggestions for Future Research . . . . .	82
Intake Passage Design . . . . .	83
Transient Air Swirl . . . . .	83
Boundary Layer Stratification . . . . .	83
Engine. . . . .	84
 BIBLIOGRAPHY	 85
 APPENDIX A HOT-WIRE ANEMOMETER TECHNIQUES	 88
Magnitude Measurements. . . . .	88
Radial Velocity Measurements. . . . .	91
 APPENDIX B SWIRL VELOCITY APPROXIMATION METHOD	 95
 APPENDIX C SWIRL GENERATION EFFICIENCY	 98
 APPENDIX D PROCEDURE FOR ESTIMATING AIR SWIRL RATE IN ACTUAL ENGINE	 100

LIST OF FIGURES

Fig. No.	Description	Page
2.1	Photograph of Flow Test Stand	15
2.2	Schematic of Flow Test Stand	16
2.3	Flow Model	17
2.4	Intake Passage	18
2.5	Calibration Setup and Air Receiver	20
2.6	Paddle Wheel Swirl Meter and Tufted Grid	22
2.7	Hot-Wire Anemometer	24
2.8	Hot-Wire Probes	25
2.9	Schematic of Hot-Wire Anemometer Circuits	26
2.10	Swirl Generators	30
2.11	External Involute Generator	31
2.12	Fin Generator	32
3.1	Effect of Shroud Arc on Air Swirl Generation for the Shrouded Valve	35
3.2	Effect of Inlet Flow Area for External Can Swirl Generator	37
3.3	Effect of Inlet Flow Area for External Involute Generator	38
3.4	Effect of Height to Width Ratio for External Involute Generator	39
3.5	Effect of Shroud Position on Air Swirl	40
3.6	Effect of Mixing Different Proportions of Straight and Swirling Flows in the External Involute Generator	42

Fig. No.	Description	Page
3.7	Effect of Mixing Valve Location Above Involute Swirl Generator	44
3.8	Static Pressure Distribution Along the Test Section	45
3.9	Air Swirl Development Along the Test Section	47
3.10	Transient Velocity Profiles	49
3.11	Transient Velocity Oscilloscope Records	50
3.12	Radial Velocity Flux at 1 Inch Radius and Static Pressure Distribution Around the Test Section	52
3.13	Effect of Unsymmetry on Flow Direction	53
3.14	Effect of Unsymmetry of Flow on Peripheral and Axial Velocities	54
3.15	Averaged Mean Flow Velocities	56
3.16	Turbulent Intensities for Shrouded Valve Generated Air Swirl	57
3.17	Turbulent Intensities for the External Involute Generated Air Swirl	59
3.18	Comparison of Turbulent Intensities	60
4.1	Description of Hypothesized and Observed Flow	66
4.2	Comparison of Perturbation Velocities	71
4.3	Effect of Volume Flow Rate on Intake Pressure Loss	75
5.1	Schematics of Swirl Generation Methods	80

Fig. No.	Description	Page
A	Wheatstone Bridge	90
B	Sample Calibration Curve for Magnitude Measurement Anemometer	90
C	Sample Calibration Curve for the IIHR Type A Hot-Wire Anemometer	94

NOMENCLATURE

Symbol	Units	Description
$A_1$	in. <sup>2</sup>	Standard intake valve lift flow area
$A_s$	in. <sup>2</sup>	Area of mixing valve admitting straight (non-swirling) flow
$A_u$	in. <sup>2</sup>	Unshrouded lift flow area for shrouded intake valve
$D/Dt$	1/sec	Substantial or material time derivative
$e$	----	Permutation index tensor
$f_i$	in./sec <sup>2</sup>	Body force term (momentum equation)
$H$	in.	Height of external involute swirl generators
$h_{wc}$	in. H <sub>2</sub> O	Wall-to-core static pressure difference
$P$	lbf/in. <sup>2</sup>	Static pressure
$P_m$	psia	Flow model chamber static pressure, absolute
$\Delta P_m$	in. Hg	Flow model chamber static pressure depression (measured from atmospheric pressure)
$r$	in.	Paddle wheel radius
$T$	msec	Time of mean transient peripheral velocity (zero time taken as arrival of axial velocity wave)
$T_{ij}^{(v)}$	lbf/in. <sup>2</sup>	Viscous stress tensor
$U$	fps	Mean flow velocity in flow direction
$U_c$	fps	Calibration air velocity

Symbol	Units	Description
$U_0$	fps	Average axial flow velocity in flow model test section (calculated from mass flow measurement)
$u'$	fps	Root mean squared turbulent perturbation velocity in the mean flow direction
$V$	fps	Mean flow velocity components
$v'$	fps	Root mean squared turbulent perturbation velocity transverse to mean flow direction (radial direction)
$\alpha$	deg	Shroud position for shrouded intake valve (measured to the shroud arc center)
$\beta$	deg	Shroud arc length for shrouded intake valve
$\gamma$	deg	Hot-wire inclination angle
$\theta$	deg	Hot-wire probe location angle (measured from the vertical)
$\mu$	lbf-sec/in. <sup>2</sup>	Absolute viscosity
$\nu$	in. <sup>2</sup> /sec	Kinematic viscosity
$\rho$	lbf/in. <sup>3</sup>	Fluid density (air)
$\phi$	deg	Flow direction azimuth (measured in the tangential direction)
$\Omega$	rad/sec	Vorticity at a point in the fluid
$\omega$	rad/sec	Vorticity at a point in the fluid evaluated for particular boundary conditions
$\omega_a$	rpm	Air rotational speed

Symbol	Units	Description
$\omega_e$	rpm	Engine Rotational speed
$\omega_p$	rpm	Paddle wheel rotational speed
$r, z, \theta$	----	Cylindrical coordinates

## I. INTRODUCTION

### 1.1 General Statement of the Problem

The term stratification refers here to the variation in the richness of the mixture in an engine cylinder. Stratification may also vary with time.

A stratified charge engine is a spark-ignited piston engine in which load control is obtained by varying the quantity of fuel only, rather than by the conventional throttling of an aspirated homogeneous mixture. Although homogeneous mixtures leaner than 0.8 of stoichiometric cannot be ignited by a conventional spark, ignitable mixtures can be obtained in "unthrottled engines" by localizing the fuel near the spark plug, that is, by stratification.

The object of employing stratification is to obtain better part load economy. This improvement results from the elimination of throttling and the associated losses, and from improvement of the cycle efficiency by approaching the air-standard cycle. The latter is a result of an increase in the rates of specific heats, with lean air-to-fuel ratios. The problems involved in a stratified engine process are those of (1) obtaining good stratification and good combustion at part load, and (2) eliminating stratification at full load when a homogeneous mixture is needed to obtain maximum output.

The present study is concerned with an engine process that intends to reconcile these contradictory requirements of part load stratification and full load homogenization by injecting fuel into a swirl generated in the engine cylinder. It is obvious that to obtain good performance the swirl will have to have a particular magnitude and character and that its magnitude and character will probably have to change with engine speed and load. It is also obvious that the swirl must be produced as efficiently as possible. It is the object of this research to investigate the feasibility of finding a simple method for controlling the air swirl rate in such a stratified charge engine and to study the mechanism of intake induced swirl generation and its effect on stratification.

Many methods of improving the part load economy of spark ignited engines have been investigated. Usually good operation was limited to only a narrow load range. In all of the investigations little, if any, cognizance was given to the actual air motion in the cylinder. Usually for engine studies greatly simplified air motion flow patterns were assumed because the accompanying turbulence made the problem too complex.

The work reported here covers investigations of the intake process on a model that was designed to resemble an actual engine as closely as possible while simulating

the intake process under steady flow conditions. Hot-wire anemometry was used to map mean steady flows, turbulent and transient flow in the model. Flow observations were conducted with paddle wheels and, visually, with a tufted grid.

### 1.2 Origin and Importance of the Study

Witzky (1)\* proposed using the phenomenon of secondary vortex flow (boundary layer induced flow) which occurs at the ends of a closed chamber containing a rotating fluid to carry the atomized fuel to the center of the chamber, thus creating stratification suitable for engine operation.

This stratification method was first observed at the University of Munich (2) where it was shown photographically that injection against the air swirl produced a fuel cloud at the center of the chamber. Later, fuel spray injection tests were conducted in a swirl chamber bomb and in a combustion bomb by Kahoun and Hussmann (3). The bombs were both designed to simulate the conditions and configurations of an actual engine combustion chamber. The conclusion reached was that the secondary vortex envisioned by Witzky as the prime agent of stratification was of secondary importance and that stratification actually came from interaction of the injected spray with

---

\*Numbers in parentheses refer to the Bibliography.

the swirling air. Simplified fuel trajectory calculations were made and comparison with fuel spray photographs indicated the development of a rich zone near the center of the chamber. For the droplet trajectory calculations the assumption of solid body air swirl was used because no air motion data were available. The results of their combustion bomb tests indicated that ignition and combustion of fuel-air mixtures as lean as 0.3 of stoichiometric overall could be obtained with a centrally located spark plug, thus proving the existence of an effective stratification mechanism.

These studies showed only that ignition of overall lean mixtures could be obtained but they did not indicate if combustion was complete or satisfactory. Engine tests aimed at determining combustion characteristics were made by Kahoun, Alperstein and Hussmann (4). They found that ignition could be obtained over a wide range of speed and load, but performance was acceptable over a limited range only.

Continued investigation of the process was conducted by Hussmann, Kahoun, and Taylor (5) in which theoretical fuel stratification or concentration maps were reported. The maps were calculated using solid body air swirl and simplified droplet evaporation laws. The maps indicated that indeed very rich fuel clouds developed near the chamber center when very small fuel quantities were

injected against the swirl. No account was made of droplet evaporation and vapor diffusion induced by turbulence in the air because turbulence data were not available. Thus, the results indicated steep fuel concentration gradients and stratification confined to rather small regions of the chamber.

The performance limitations of the "swirl induced" stratified charge engine are due mainly to insufficient control of the fuel trajectories. The process depends on the interaction of the fuel spray with the swirling air. Since very little control can be exercised over the spray characteristics for a given nozzle, control of the air swirl becomes attractive. Therefore, it is important to learn what the characteristics of the existing air swirl are, determine the swirl requirements of the combustion process, and to find adequate and possibly adjustable means of providing the proper swirl.

### 1.3 Previous Related Studies

Many methods have been used to produce an intake induced air swirl in engines. The shrouded or masked intake valve was perhaps the first method and one which is still being used because of its simplicity. Most of the experimental work reported on air motion in an engine cylinder has been conducted on compression ignition engines. In such engines improved mixing and

combustion result from induced air motion without resort to complex chamber design. The one common result reported in all investigations is that for any given configuration, the swirl rate (air revolutions per engine revolution) is nearly constant over a large range of engine speeds.

Several swirl generation methods are presently used in production engines and there is much controversy about their relative merits. The controversy comes from the fact that each designer chooses a different method based on incomplete information and no valid method of comparison is available. Meurer (6) uses a snail shaped intake passage. Core design and production of such a passage is very difficult. Wittek (7) uses shrouded valves to produce swirl. He employs dual valves to overcome the volumetric efficiency problem, but costs are thereby increased. Others are using such devices as tangential inlet ports and masks or by partially blocking the intake passage near the valve opening to restrict the air flow on one side.

#### Engine Studies

One of the early investigators of the actual air motion in an engine was Ricardo (8) who conducted tests with a paddle wheel vane inside the cylinder of a motored engine. The vane speed was recorded with a directly connected revolution counter and the air drag

on the paddles provided the torque to drive the counter. His investigations were in a sleeve-valve compression ignition engine. The paddles were flat and extended to all regions of the clearance volume, thus the results reported were of an integrated nature.

A very comprehensive investigation on swirl studies, using the vane method to measure swirl rate, was reported by Alcock (9). His measurements were conducted in a cup-type open chamber where the swirl was intake induced; and in a Ricardo prechamber where the swirl was compression induced. It was concluded that high swirl rates were difficult to achieve with a poppet valve system. A discussion to his paper described attempts to map the air motion in an engine using a pitot tube. Alcock's report (1934) describes the existence of the secondary vortex caused by friction at the end walls and points to the analogy with the motion of tea leaves at the bottom of a stirred cup of tea.

Lee (10) in 1939 presented one of the few reports on nonintegrated air motion studies in spark ignited engines. His purpose was to study the effect of swirl on improving performance of an engine using gasoline injection during the intake stroke. Feathers were introduced into the intake air and photographed through a glass cylinder with a high speed camera to record the air motion. He states that

"a wide variety of induced movements could be created all of which persisted through the compression stroke but only rotation about the cylinder axis continued into the expansion stroke".

#### Steady Flow Model Studies

Percival (11) conducted measurements under steady flow conditions in a model cylinder in which the piston was held stationary for purpose of studying the effect of swirl on scavenging in a uniflow diesel. The flow was mapped with an aerodynamically calibrated sphere-shaped pressure probe. Similar experiments were conducted on a model cylinder containing the stationary piston of the same engine by Sobel (12) using paddle wheels to map the swirl. The results of both methods agreed quite well. Later, Law and Hussmann (13) conducted extensive swirl mapping also by the paddle wheel technique in a similar model cylinder setup of the same engine for the purpose of producing high swirl rates.

Recently, Pischinger (14) reported results of a model study where swirling flows were mapped with a paddle wheel. He presents justification for the application of the results from a steady state flow model to the transient process of the engine by equating the integrated flows in the engine and model.

Pischinger's results for shrouded-valve generated swirl agree quite well with those obtained in this investigation.

#### 1.4 Specific Statement of the Problem

The purpose of this investigation was to examine by model studies the air motion in the engine cylinder and to study the mechanism of intake induced air swirl in the engine.

#### Hypothesis to be Investigated

Previous investigations of the Witzky stratified charge system by Kahoun et al. (3) assumed a symmetrical air swirl profile with turbulence neglected. His spray chamber and combustion bomb were both constructed to provide such a flow.

In the engine, however, the situation is quite different. The incoming air must flow around a bend in the intake passage. The intake valve is not symmetrically located because space must also be provided for the exhaust valve. If a shrouded valve is used to produce the swirl, it produces additional unsymmetry of the flow by deflecting the incoming air in one direction. Intake system transients and pressure pulsations common in branched manifolds could possibly affect the cycle-to-cycle strength of the generated swirl. The presence of residual gases and their motion must also be considered.

Consideration of the aforementioned engine complexities and the phenomena of "swirl induced" fuel stratification led to the following hypothesis: If an air swirl is generated by separate means ahead of the

intake valve a more organized and stable swirl will develop and this will result in a lower turbulence level.

#### Air Swirl Control

Air swirl velocity and flow pattern exert a great influence on engine performance by affecting fuel trajectory. The main problem comes from the fact that the quantity of the injected fuel also influences the ease with which a spray is deflected by the air motion existing in the engine cylinder. Since it is very desirable to use only a single spark plug, it is important that the fuel reaches the same region of the chamber at all possible combinations of speed and load. Because it is impractical to vary the spray characteristics, it would be advantageous to have a simple mechanism for varying the air swirl velocity.

The ability to control the swirl velocity or rate should provide several advantages. The fuel trajectories could be controlled independently of the fuel quantity or engine speed. The loss in volumetric efficiency caused by the energy required to produce the swirl, could be eliminated where no swirl is required. Reduction of the volumetric efficiency loss is not possible with the shrouded valve because shroud position (which can be used to control swirl rate) affects it only slightly.

#### Turbulence

Turbulent motion is a form of irreversible energy

dissipation that can be created by inducing high shear rates in a viscous fluid. A high level of air turbulence (random motion) is desirable in engines because of the advantages it provides to fuel evaporation, distribution and combustion. Mechanisms such as squish and swirl are often used to provide the needed turbulence.

In the stratified charge engine it is desired ideally to have a localized patch of chemically correct fuel-air mixture in which combustion is rapid and complete. Load would then be varied by the size of the patch. This ideal is not attained because the existence of turbulence tends to flatten and spread the fuel concentration profile. A reduction of turbulence at part load would assist in maintaining steep concentration gradients while probably not interfering significantly with performance particularly at full load.

At or near full load fuel concentration gradients can be tolerated more readily and may even be of advantage because lean end-gas regions tend to reduce knock. These lean regions should, however, not be so lean that combustion is slowed excessively or quenched. This was discussed in detail by Schweitzer (15).

### 1.5 Scope and Limitation of the Study

The purpose of the investigation was to investigate the mechanism of intake induced air swirl generation and the possibility of providing a simple method of con-

trolling air swirl in a stratified charge engine. The study was conducted on a flow model designed to simulate under steady flow conditions, the intake process of an actual engine.

Study of the transients affecting the intake process was limited, because such transient flow measurements are very difficult to make. The injection of a fuel spray into the swirling air of the model would not produce the same trajectory as it does in the engine because of the large differences in air densities. A study of the contribution of boundary layer (secondary vortex) stratification as proposed by Witzky (1) was not possible because the steady flow apparatus produces near the inlet valve a very different flow pattern than exists in the engine after valve closure.

## II. PROCEDURE OF THE INVESTIGATION

### 2.1 Model Design

The "swirl induced" stratified charge system as proposed by Witzky (1) was investigated on an engine by Kahoun, Alperstein, and Hussmann (4). The engine used in their investigations was supplied by White Motor Company of Cleveland, Ohio and consisted of a REO-V-8 gasoline engine with only one operating cylinder. A special two-valve diesel cylinder head designed by White was modified to adapt it to the stratified charge system. The intake valve was shrouded to provide the necessary air swirl.

At the outset it was decided that the model for the study of the intake induced swirl should be constructed to resemble the experimental engine as closely as possible. This would provide maximum correlation between model and engine and facilitate application of the findings.

A plaster model of the cylinder head containing only the intake passage was produced by the lost wax method. Great care was taken in forming the wax core in accordance with intake passage drawings furnished by White Motor Company. Plan and section views of the intake passage are shown in Fig. 2.4.

### 2.2 Experimental Apparatus

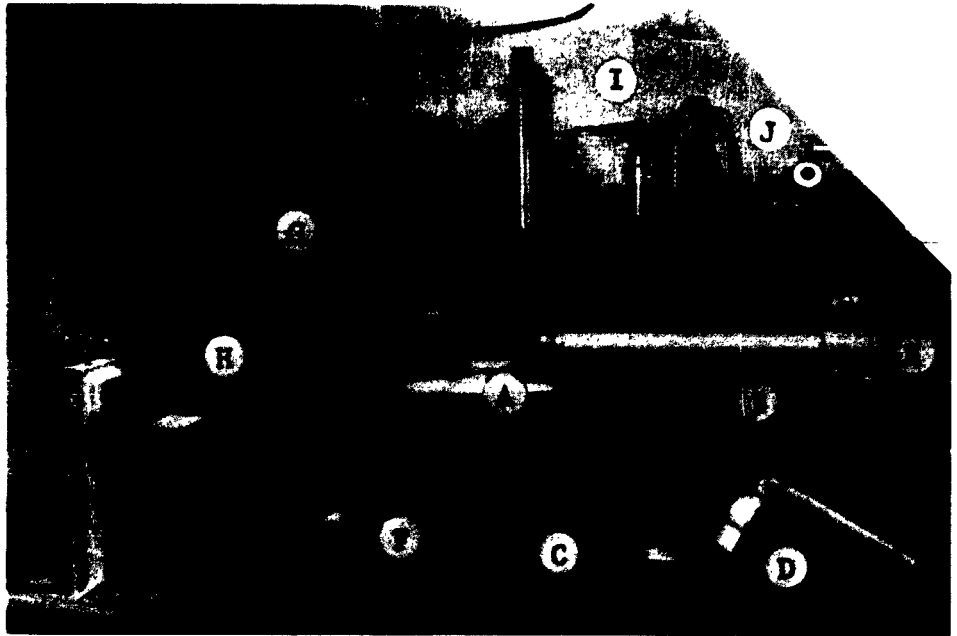
Figure 2.1 is a photograph and Fig. 2.2 is a

schematic of the experimental apparatus. The flow stand consisted of a model (see Fig. 2.3) of the engine head and cylinder with the intake passage shaped in plaster. A Rootes blower that had served as the scavenging pump on a General Motors 4-71 diesel engine was used to draw air through the apparatus. The blower was driven by a 5 HP induction motor at a nominal speed of 1725 rpm. At this speed the blower developed 15 in. Hg suction at zero flow and pumped approximately 160 cfm without flow restriction.

The air flow through the model was varied by introducing bypass air upstream of the blower.

The three-lobe construction of the blower induced pressure pulsations of about 90 cps into the flow and therefore a 10 ft<sup>3</sup> plenum chamber was provided to dampen the pulsations. The plenum chamber also acted as a safety device by preventing the blowing of manometers when starting and stopping the blower. The blower exhausted to the atmosphere. The exhaust pulsations produced considerable noise when any significant suction was developed by the blower; a truck engine muffler was used to attenuate this noise.

The flow model, as discussed before, was designed to simulate the intake stroke of the engine under equivalent steady flow conditions. Therefore, the air receiver (shown in Fig. 2.5) was designed to prevent penetration



- A Flow Model
- B Air Receiver
- C Calibration Setup
- D Short Air Receiver
- E Modified Gate Valve
- F Make-up Air Valve
- G Plenum Chamber
- H Blower
- I Manometers
- J Barometer

FIG. 2.1 PHOTOGRAPH OF FLOW TEST STAND

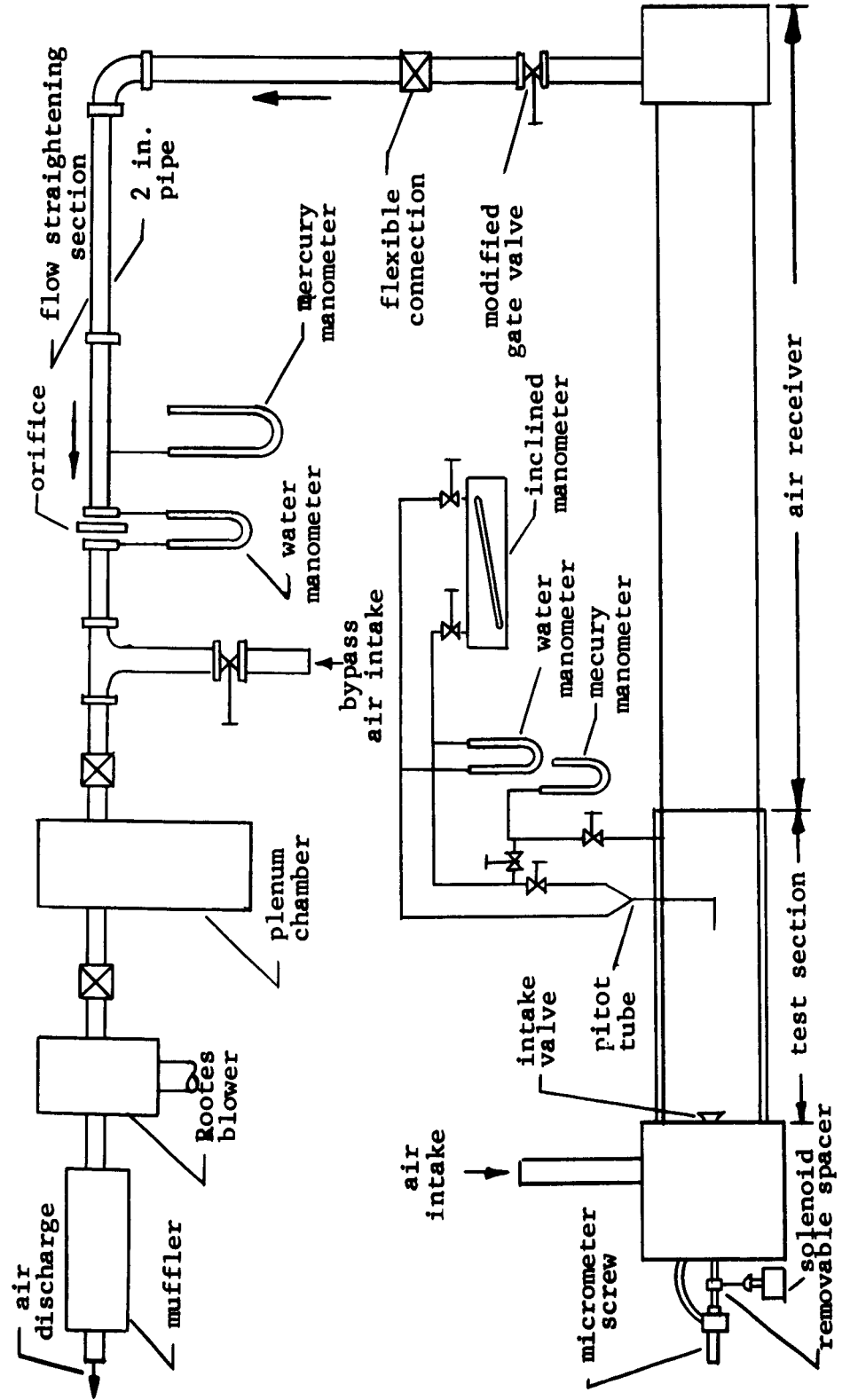


FIG. 2.2 SCHEMATIC OF FLOW TEST STAND

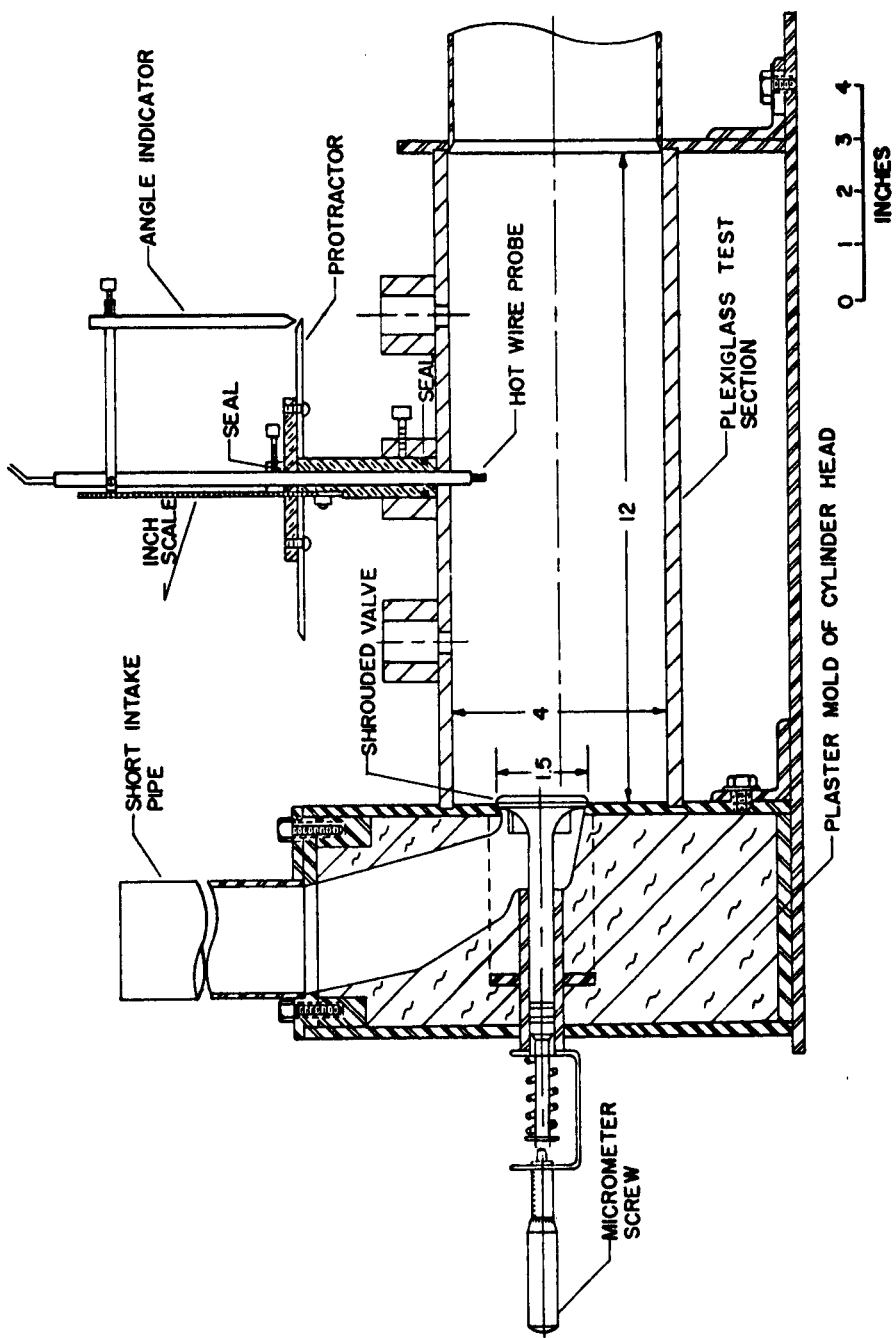


FIG. 2.3 FLOW MODEL

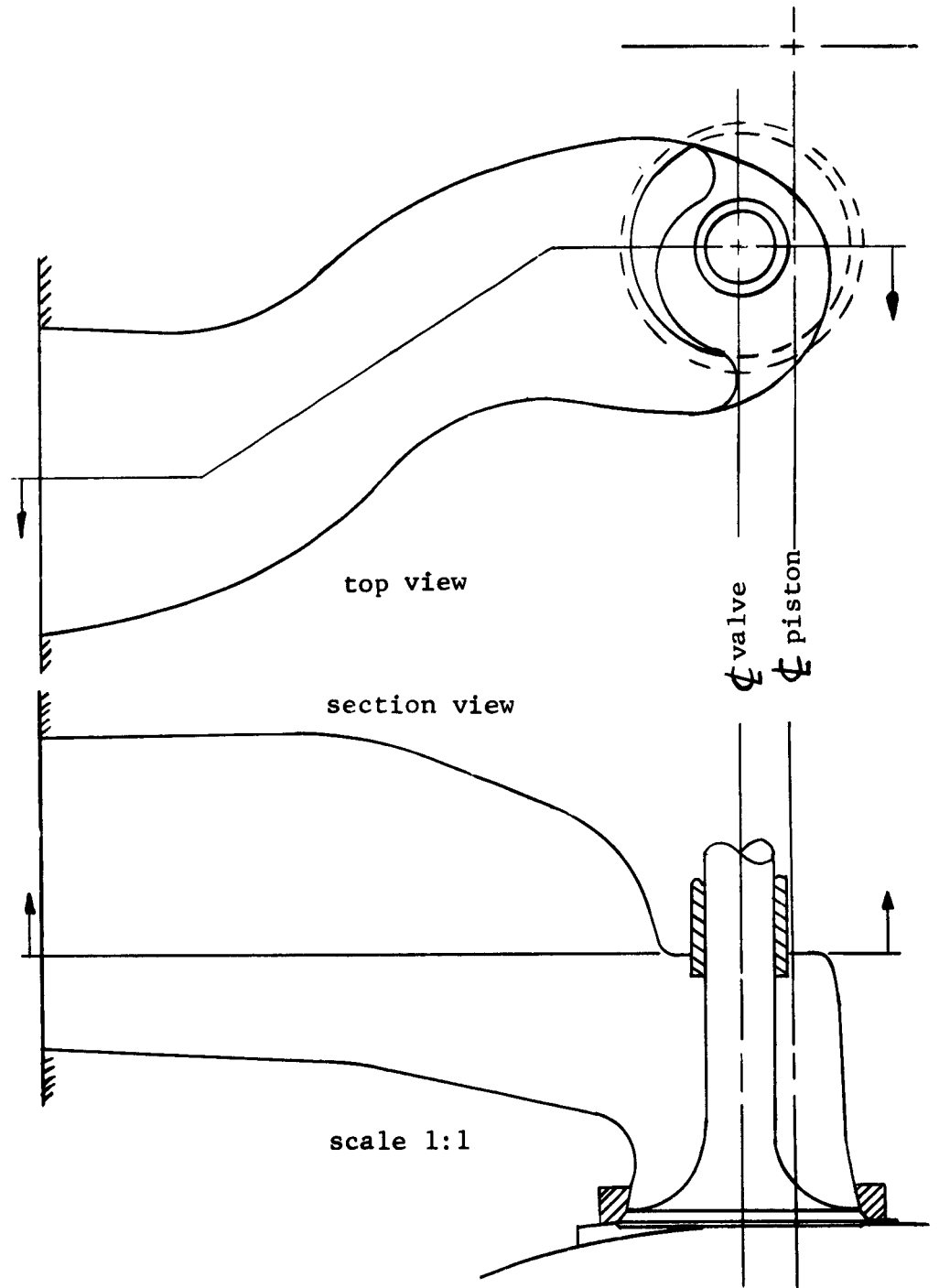


FIG. 2.4 INTAKE PASSAGE

of outflow disturbances back into the test section. This was accomplished by providing baffles and flow restrictions to produce uniform sink flow and by removing the outflow a significant distance from the test section.

A very serious problem that often plagues users of hot-wire anemometers is the problem of mechanical vibrations that bend or break the wires. This problem was solved by supporting the blower and motor platform on a 4 in. cork pad; providing flexible rubber hose connections in the 2 in. line on both sides of plenum chamber and at the exhaust from the air receiver, and mounting the flow model and the air receiver on 2 in. foam rubber pads.

The mass flow through the model was measured with a sharp edged orifice flowmeter. A standard stainless steel orifice plate with a concentric hole ( $\beta = 0.7$ ) purchased from the Meriam Instrument Company was used. The pressure taps were positioned and a calibration curve was constructed according to the A.S.M.E. Flowmeter Handbook. Because the flow model generated a swirl in the pipe it was necessary to provide a flow straightening section ahead of the orifice meter. This section consisted of a bundle of thin wall copper tubes, 2 ft long, 3/8 in. in diameter, brazed together and placed in the 2 in. line about 15 diameters ahead of the orifice meter.

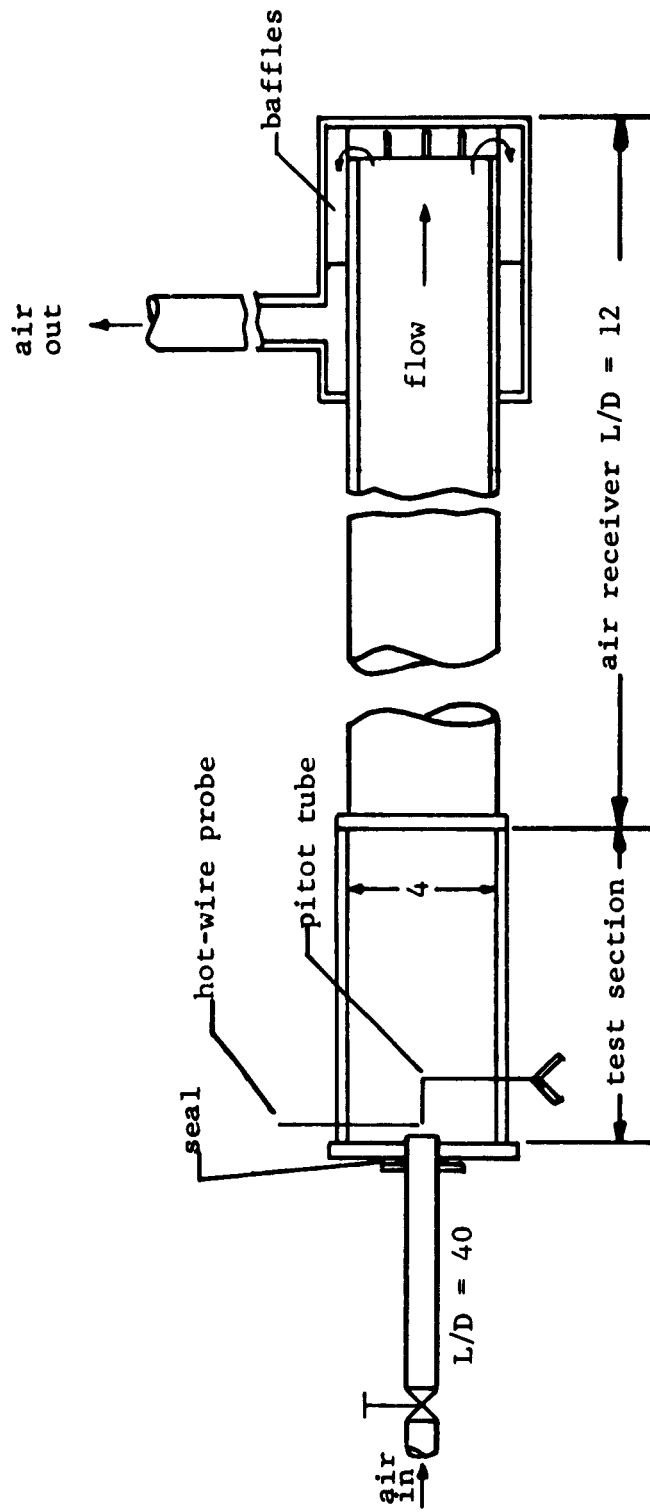


FIG. 2.5 CALIBRATION SETUP AND AIR RECEIVER

### 2.3 Flow Investigations

#### Qualitative Observations

Visual observation of the air flow in the test section was conducted by use of a tufted grid and paddle wheels (shown in Fig. 2.6). To accommodate these observations a shorter air receiver was constructed. The paddle wheels were mounted on a long polished shaft 1/16 in. in diameter to reduce friction. Very small Teflon bearings were used also to reduce friction and the paddle wheels were carefully balanced. The Teflon bearings were about 1/16 in. long and were machined to shaft size after they were glued into the paddle wheel hub. The paddle wheel speed was measured by observing with a Strobotac the one paddle that had been painted black.

#### Flow Mapping

Accurate mapping of swirling flows in a circular duct is a difficult problem. Percival (11) used a very small aerodynamically calibrated pressure probe which was quite good, but the labor involved in getting adequate data was tremendous. His method would also have some error in mapping turbulent flows because the static pressure point on a sphere or cylinder is affected by the level of turbulence.

There is also the possibility of sensing only the total pressure and flow direction and extrapolating the

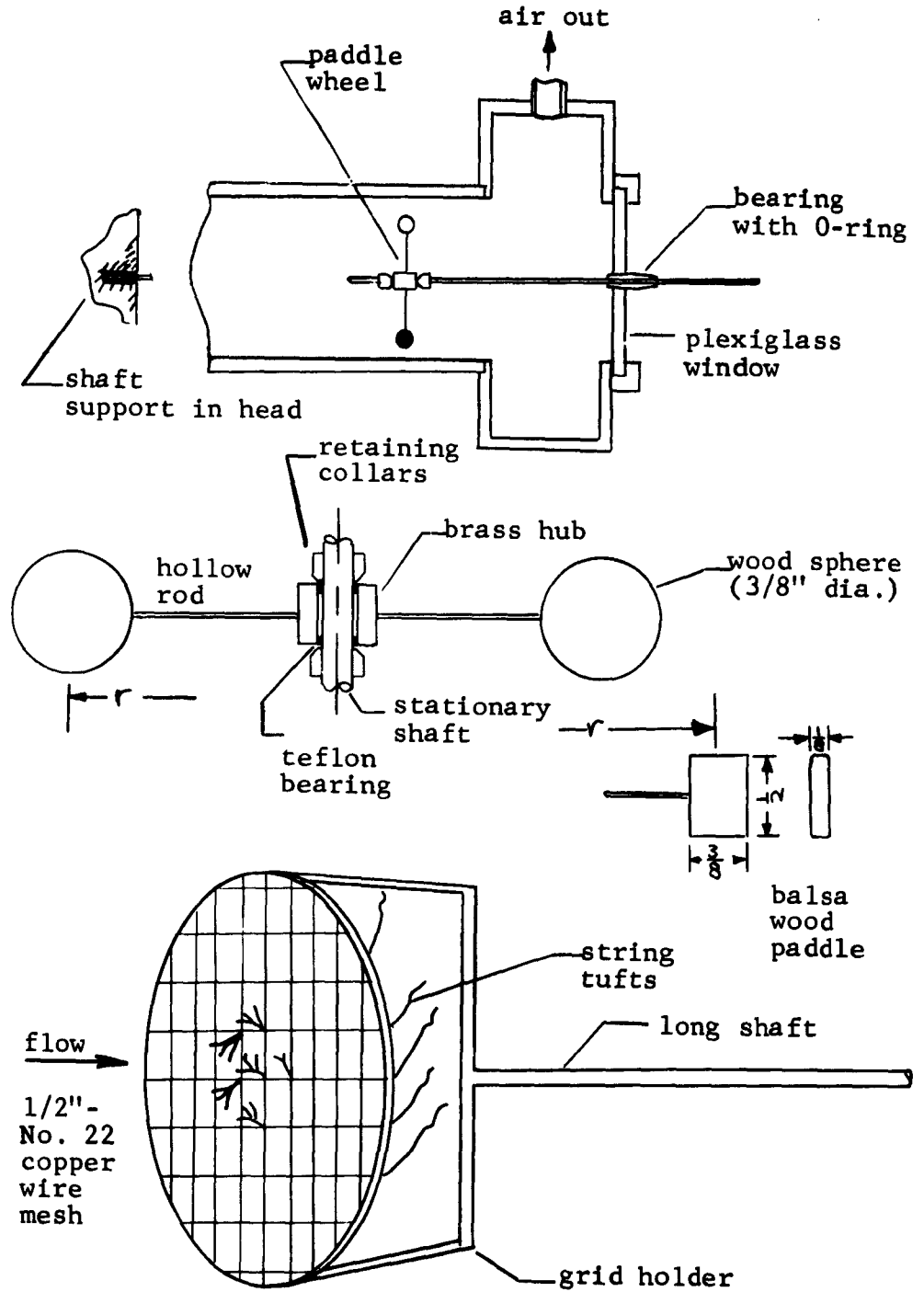


Fig. 2.6 PADDLE WHEEL SWIRL METER AND TUFTED GRID

static pressure from the wall by the method as proposed by Maybach (15). This too is very laborous. Attempts by Holman and Moore (16) to measure pressures in a vortex chamber introduced errors as large as 50% by the presence of the probe alone. Meurer (6) and Pischinger (14) used the paddle wheel technique but it does not give a complete picture. Because of the complex nature of the induced swirl flow in a poppet valve engine, the hot-wire anemometer technique was selected.

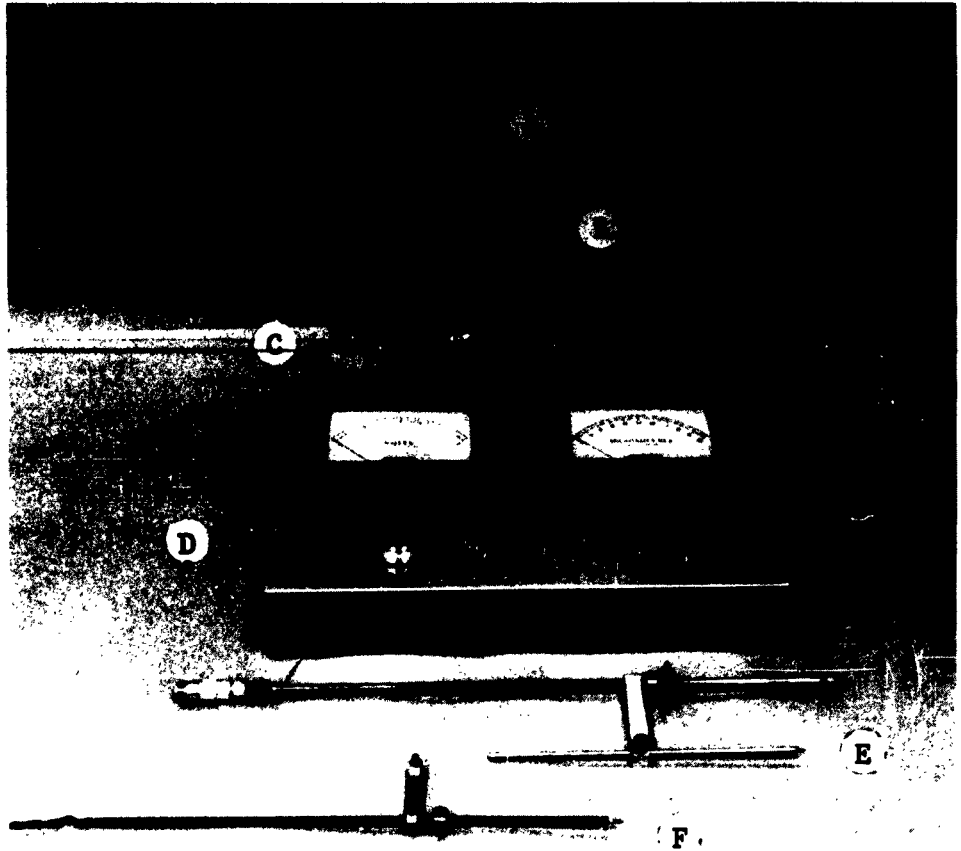
A velocity magnitude measuring hot-wire anemometers was developed and constructed using the principle of an unbalanced Wheatstone bridge (17). (see Figs. 2.7 thru 2.9) The anemometer design is discussed in detail and a sample calibration curve is given in Appendix A.

#### Calibration

A special setup was constructed (shown in Fig. 2.5) to permit calibrating the anemometer for the same conditions under which it was used. By combined adjustments of the valve on the calibration setup and the valve on the bypass air line, both the flow velocity and air density could be varied. The air temperature was measured with a thermocouple located near the hot wire (see Fig. 2.8).

#### Azimuth Measurements

The single hot wire when held normal to the air flow is sensitive to magnitude only. When it is turned it be-



- A Azimuth Measurement Probe
- B Probe Holder and Angle Indicator
- C Test Section
- D Anemometer
- E Turbulence Measurement Probe
- F Magnitude Measurement Probe

FIG. 2.7 HOT-WIRE ANEMOMETER

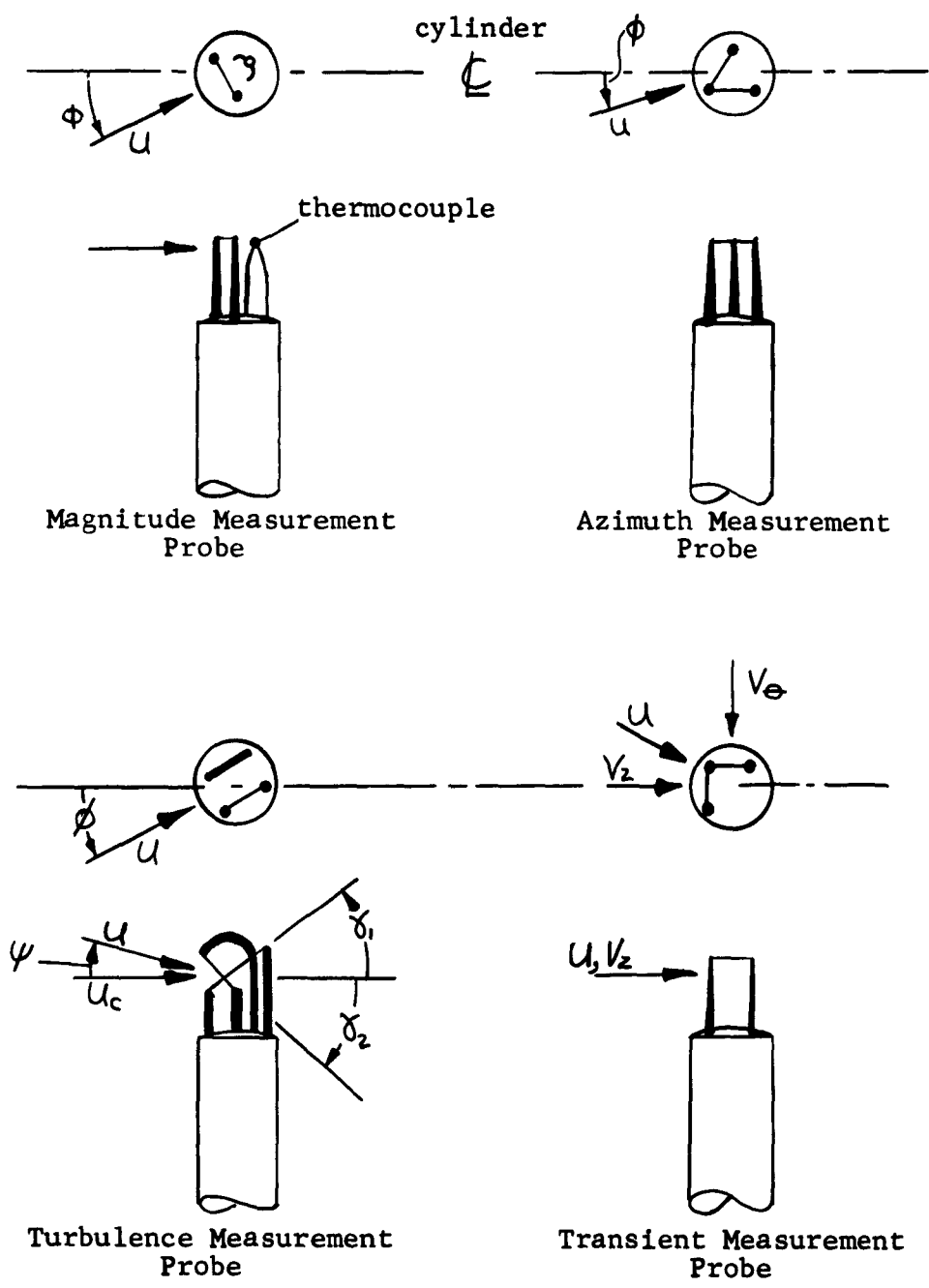
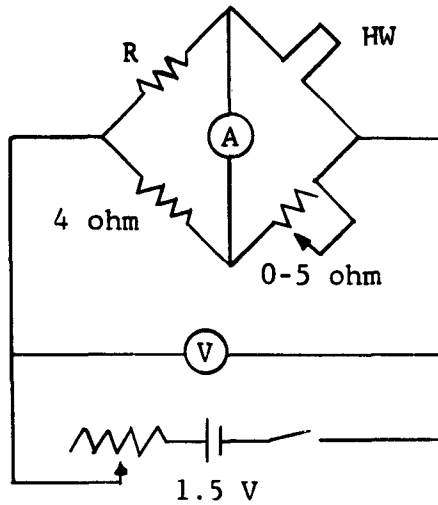
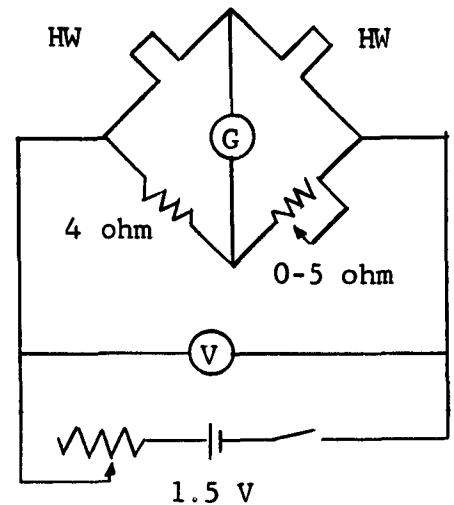


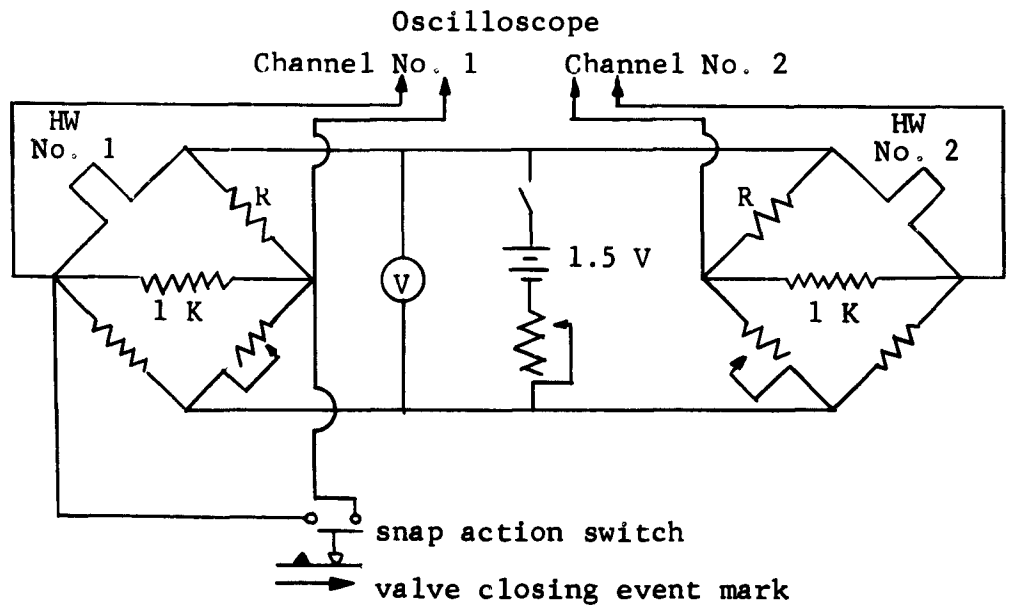
FIG. 2.8 HOT-WIRE PROBES



Magnitude Measurement Circuit



Azimuth Measurement Circuit



Transient Velocity Circuit

Note: R : Hand wound Karma wire resistor, 1.20 ohms.  
 HW : 1-mil platinum hot wire, 0.75 ohms.

FIG. 2.9 SCHEMATIC OF HOT-WIRE ANEMOMETER CIRCUITS

comes sensitive to direction. The investigation effort was simplified greatly by constructing an azimuth measuring probe (Fig. 2.8). The device consisted of two wires inclined at equal angles to the flow in the tangential direction. The two wires formed two legs of a bridge circuit (Fig. 2.9). When the bridge was balanced the flow direction was known. This setup was calibrated and checked at all velocities and it was found to be accurate to within  $1^\circ$ .

#### Radial Velocity Measurements

The turbulence measuring probe shown in Fig. 2.8 was constructed of two hot wires which were inclined to the flow in the radial direction. This made the probe sensitive to radial velocities. A method is worked out in Appendix A to measure the radial angle and the radial velocity.

#### 2.4 Turbulence Investigations

The turbulence measurements conducted for this investigation were taken with the II HR Type A Hot-Wire Anemometer. A cross wire probe as shown in Fig. 2.8 was constructed for the measurements. The wire used was 0.00012 inch diameter Tungsten with a 10% platinum coating which was then copper plated to a size easy to handle. After the wires were soldered in place the copper was etched away until the wire had the required 5 ohms resistance. Complete description of probe

construction and shortcut techniques is discussed in detail by Margolis (18). A sample calibration curve for the anemometer is shown in Fig. C of Appendix A. The operating of the anemometer and the calibration of turbulence data is covered in detail by Hubbard (19).

### 2.5 Transient Flow Studies

A hot wire network (Fig. 2.9) was used to map the decay of the air swirl. A quick closing gate valve was installed in the exhaust line from the model (Fig. 2.2). A special block was used to prop the intake valve open and an electric solenoid was used to automatically release the block while simultaneously closing the gate valve. The hot wire anemometer was orientated so that one wire measured the peripheral velocity ( $V_{\theta}$ ) and the other measured the axial velocity component ( $V_z$ ) (see Fig. 2.8). Decay times were measured using the arrival of the valve-closing wave at the probe as the base or zero time. The oscilloscope traces were recorded with an oscilloscope film strip recorder. A snap action switch was used to signal the valve closing event for ease in determining the time of events on the film strip.

### 2.6 Swirl Generators

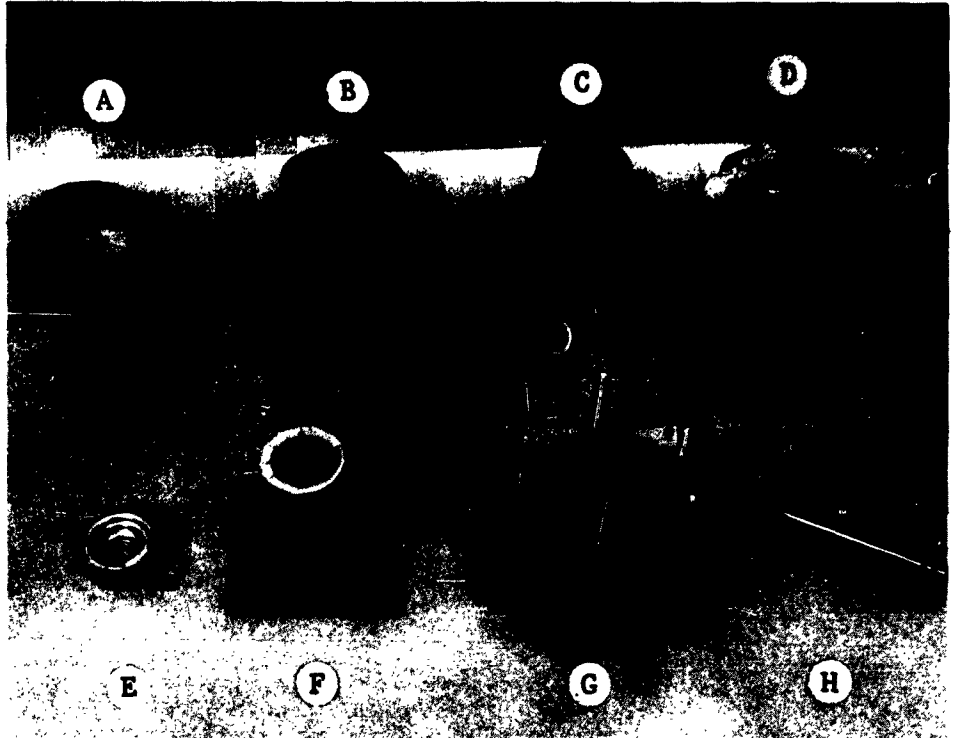
Four different methods of air swirl generation were employed. In addition the standard shrouded intake

valve method, the investigation included considerations of three other methods.

The shrouded intake valve was investigated first because it was being used on the engine. It was felt that a thorough understanding of the method that made the system operable would help greatly in understanding the problems with the system. The shrouded valve was also used throughout the investigation as a reference for comparison. A special shrouded valve was constructed of aluminum for the purpose of studying the effect of shroud arc over a large range. This was done by cutting sections of the shroud away after each test.

The problem of variable rate swirl generation was first approached by studying external swirl generation. For this the external (tangential) can generator (see Fig. 2.10) was constructed and tested. The results of these tests indicated that a study of generator geometry should be considered.

A device was constructed to hold an involute shaped sheet metal wall between two flat surfaces (involute generator, see Fig. 2.10 and 2.11). With this device families of shapes and sizes of swirl generators could be studied by simply bending a new piece of sheet metal. Shown in Fig. 2.10 are the sheet metal walls used to vary the generator height ( $H$ ), the generator inlet width ( $W$ ), and the generator inlet height to width



- A External Involute Walls (Variable Inlet Width)
- B External Involute Walls (Variable Inlet Height)
- C External Involute Walls (Constant Inlet Area)
- D External Can
- E Concentric Disc (Mixing Valve)
- F Adaptor (Used to Mix Straight Flow)
- G External Involute (Optimum Configuration)
- H Shrouded Valve

FIG. 2.10 SWIRL GENERATORS

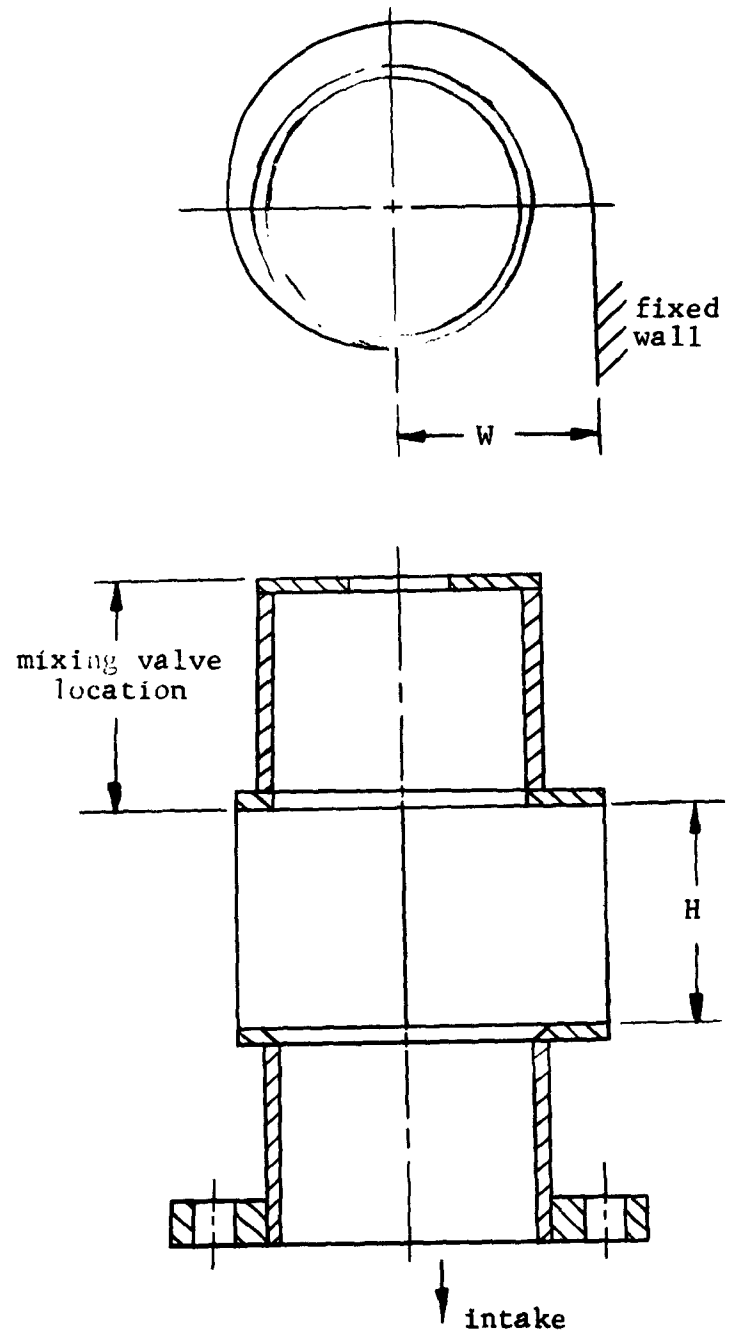


FIG. 2.11 INVOLUTE SWIRL GENERATOR

Optimum Configuration

$W = 1.80$  in.

$H = 1.25$  in.

Mixing Valve Location = 0.0 in.

(H/W). After this generator was optimized (Fig. 2.10 and 2.11) the resulting shape was used for all subsequent testing.

For the purpose of studying swirl generation in the direction of the cylinder axis upstream of the intake valve, a fin generator was constructed and installed in the intake passage just ahead of the valve (see Fig. 2.12). The fin was cut and shaped from thin metal and held in place with putty. Since the intake passage was not designed properly for this method of swirl generation, only preliminary studies of it could be conducted.

The intake valve lift on the White engine was measured with a dial indicator. The lift was then plotted against crank angle and integrated to find the average. This average (0.288 in.) was then used as the lift setting on the model for all testing.

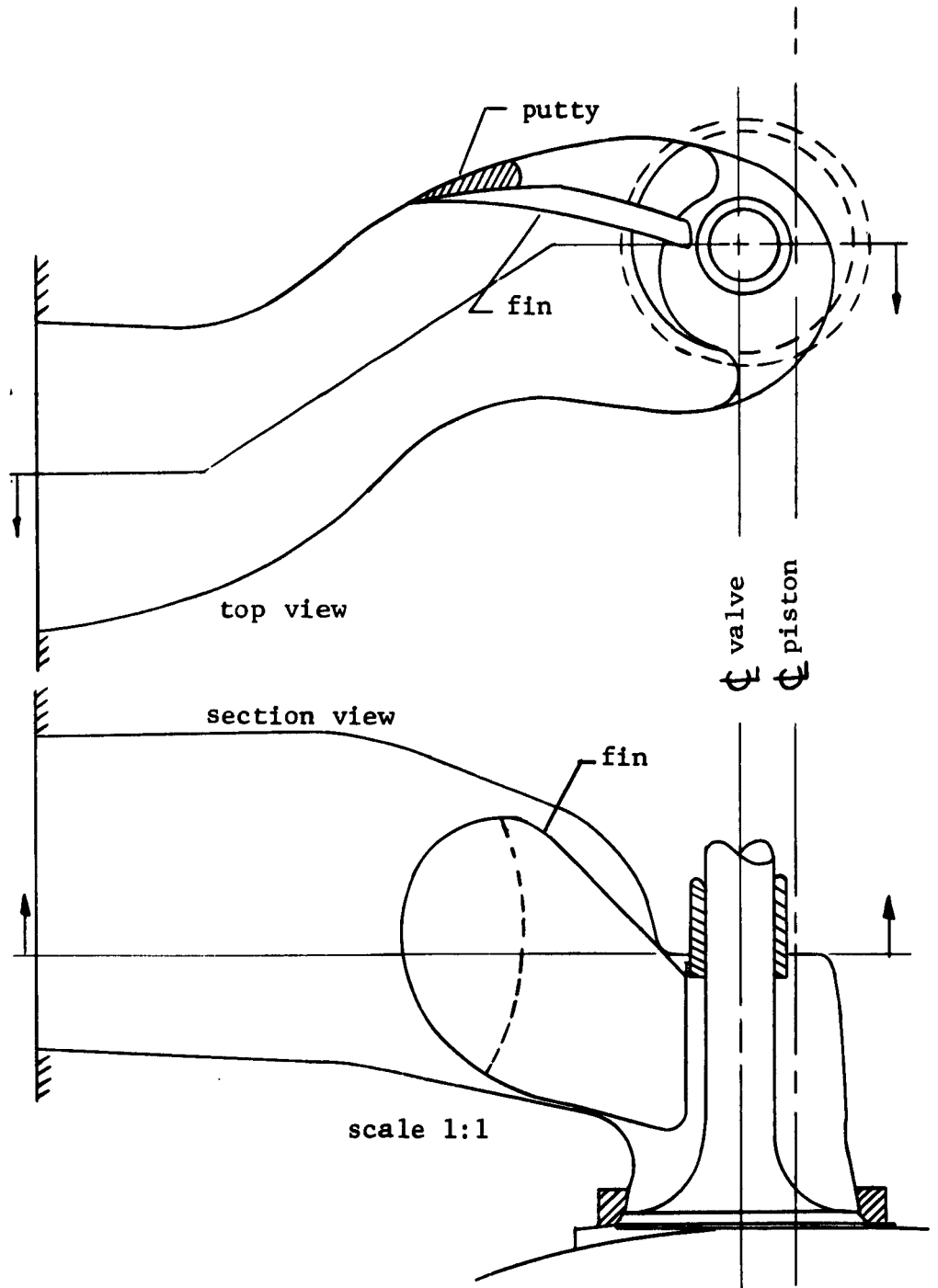


FIG. 2.12 FIN GENERATOR

### III. EXPERIMENTAL RESULTS

From observation of the tufted grid in the swirling air stream of the model it was noted that the air flow along the test section wall spiraled generally downward toward the model exit. These observations also indicated a reverse flow in the core of the swirl. The reverse flow region became increasingly larger as the tufted grid was moved toward the head of the model and was largest when the grid was in the wake of the intake valve. Some of the tufts as shown in Fig. 2.6 illustrate this situation. The tufted grid observations also indicated the existence of a very high level of turbulence throughout.

#### 3.1 Geometric Investigations

Figure 3.1 shows the effect of various shroud arc lengths with shrouded valve swirl generation. These results were obtained by successively removing sections of the shroud to vary the shroud arc. During each test the shroud was rotated to give maximum swirl (maximum wall-to-core static pressure difference). This shroud position for maximum swirl was very nearly constant ( $\pm 10^\circ$ ) for all shroud arcs. From the measured wall-to-core pressure ( $h_{wc}$ ) and the chamber static pressure depression ( $\Delta P_m$ ) the air swirl velocity ( $\omega_a$ ) was calculated by considering non-viscous, two dimensionally symmetric, solid body flow.

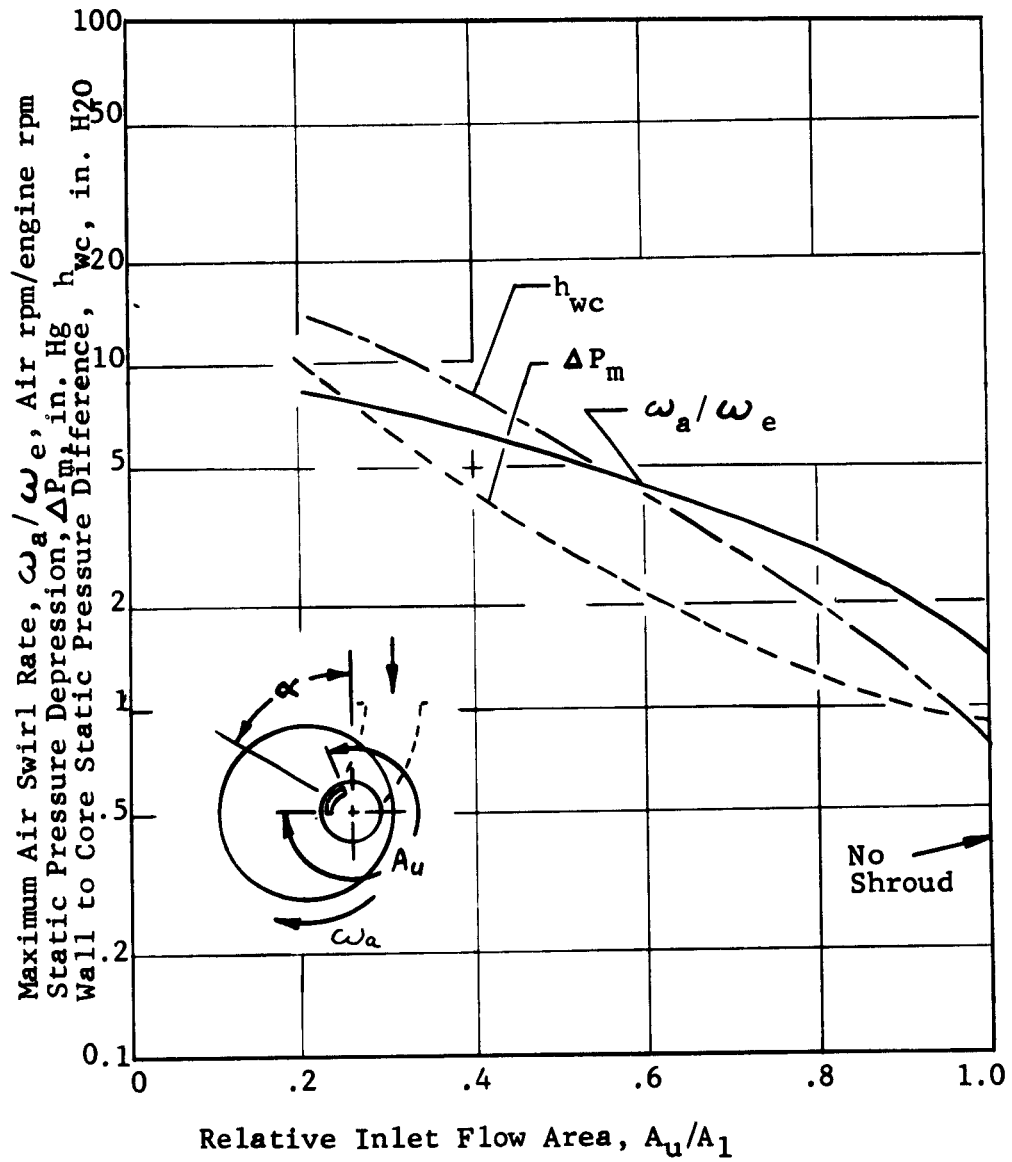


FIG. 3.1 EFFECT OF SHROUD ARC ON AIR SWIRL GENERATION FOR THE SHROUDED VALVE

- $h_{wc}$  = Measured 9 in. from Head
- $\alpha$  = Shroud Arc
- $U_o$  = 19.1 fps (Average Axial Velocity in Test Section)
- $A_u$  = Unshrouded Area
- $A_1$  = Total Lift Area
- $\alpha$  = Shroud Position

This procedure is outlined in Appendix B. The engine speed ( $\omega_e$ ) was used to rationalize the model results and was taken as the speed required to produce the same rate of piston displacement as the volume flow through the model test section. Figure 3.1 indicates that the unshrouded valve also produced some swirl which was apparently caused by the shape of the intake passage. The effect of shroud position on air swirl is shown in Fig. 3.5.

Preliminary investigations on generation of an air swirl external to the intake were conducted with the external (tangential) can device (shown in Fig. 2.10). The results of this test (shown in Fig. 3.2) indicated a very high swirl rate, but at the expense of an extremely high pressure loss ( $\Delta P_m$ ). This observation led to the investigation of external swirl generator geometry (Figs. 3.3 and 3.4). The optimized external swirl generator was then found from the results of Fig. 3.4 (an involute configuration) and is shown pictorially in Figs. 2.10 and 2.11.

### 3.2 Air Swirl Rate Control

The only possible method of controlling the air swirl rate in an engine using a shrouded valve as a swirl generator is that of rotating the intake valve to change the shroud position. Figure 3.5 shows the effect of shroud position on air swirl in the model. This method

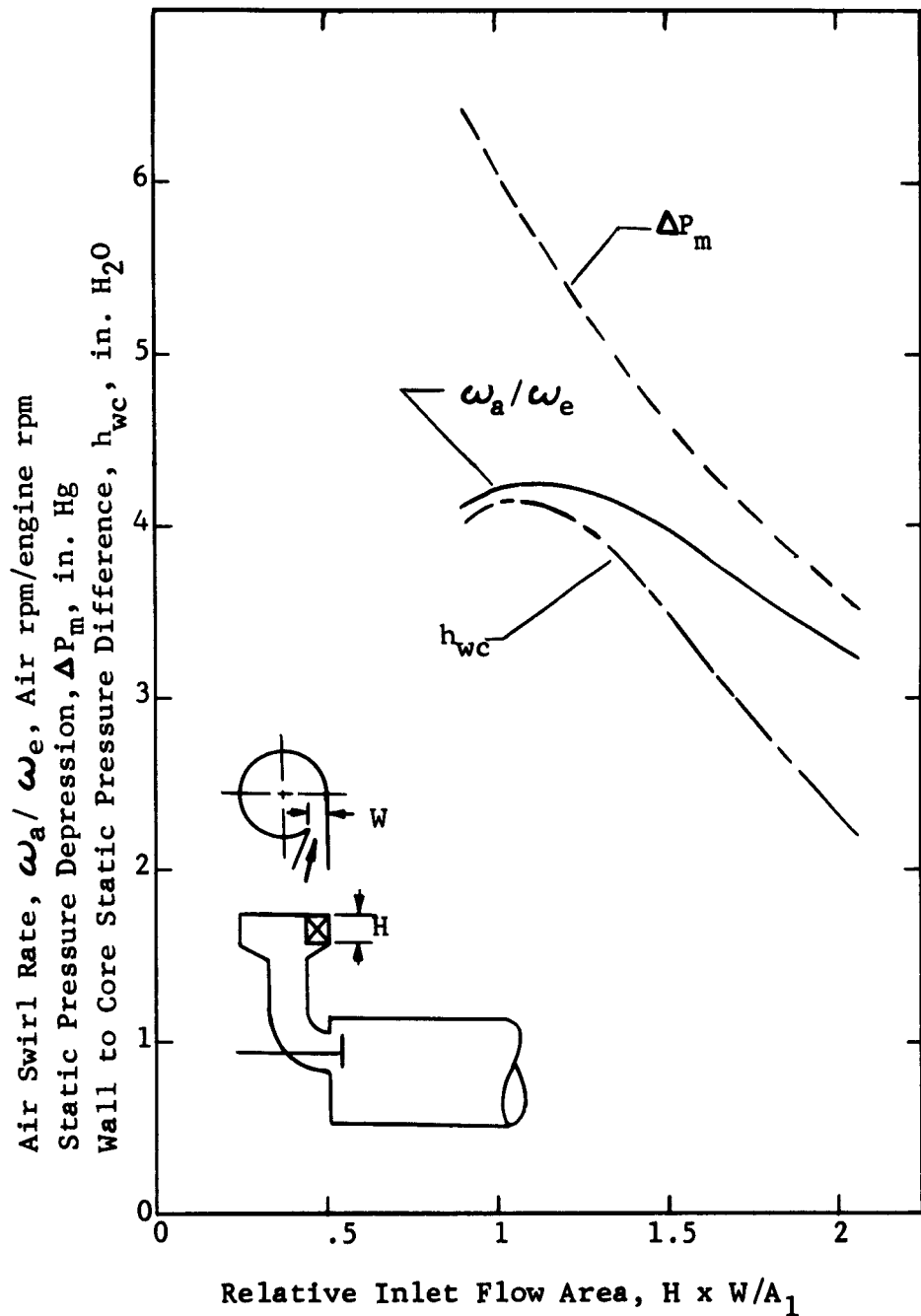


FIG. 3.2 EFFECT OF INLET FLOW AREA FOR THE EXTERNAL CAN SWIRL GENERATOR  
 $U_o = 19.1$  fps  
 $H =$  Height = 1.50 in.  
 $W =$  Width of Inlet  
 $A =$  Lift Area of Inlet Valve

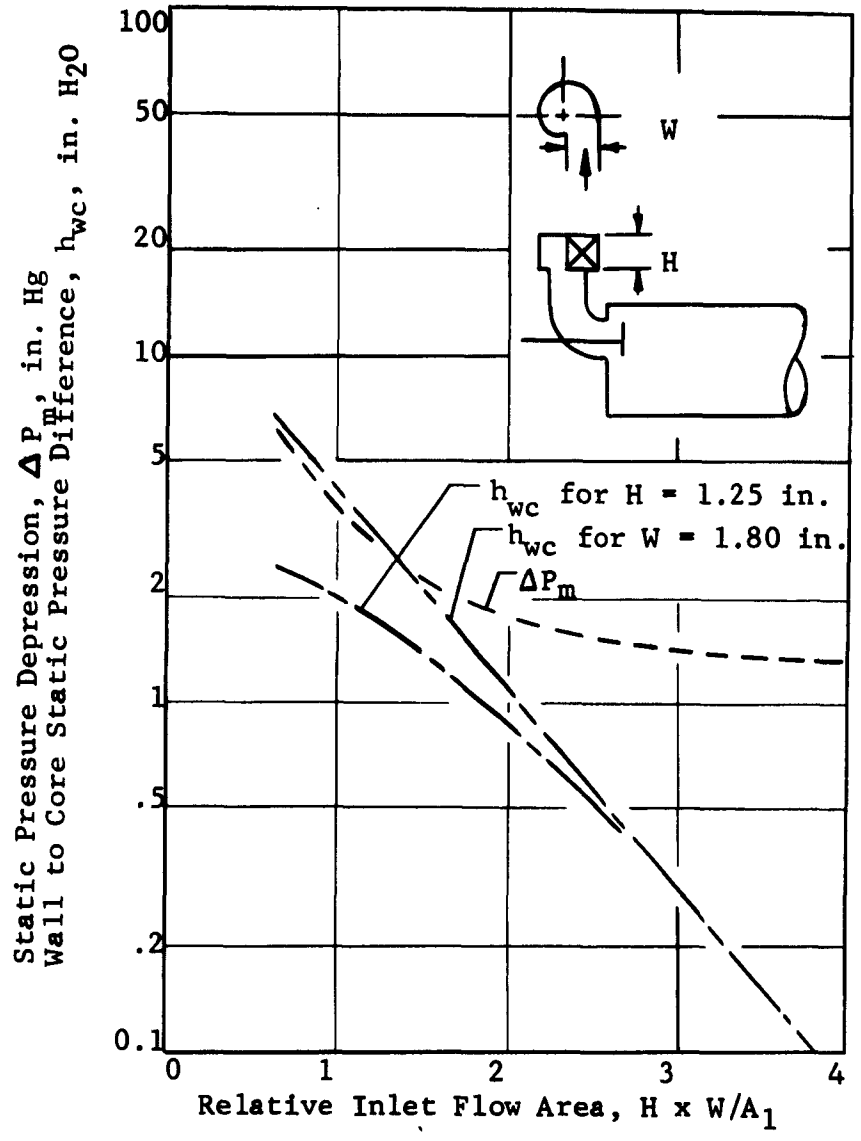


FIG. 3.3 EFFECT OF INLET FLOW AREA FOR EXTERNAL INVOLUTE GENERATOR

- $U_o = 19.1$  fps
- $H =$  Height of Generator
- $W =$  Width of Inlet
- $A_1 =$  Lift Area of Inlet Valve

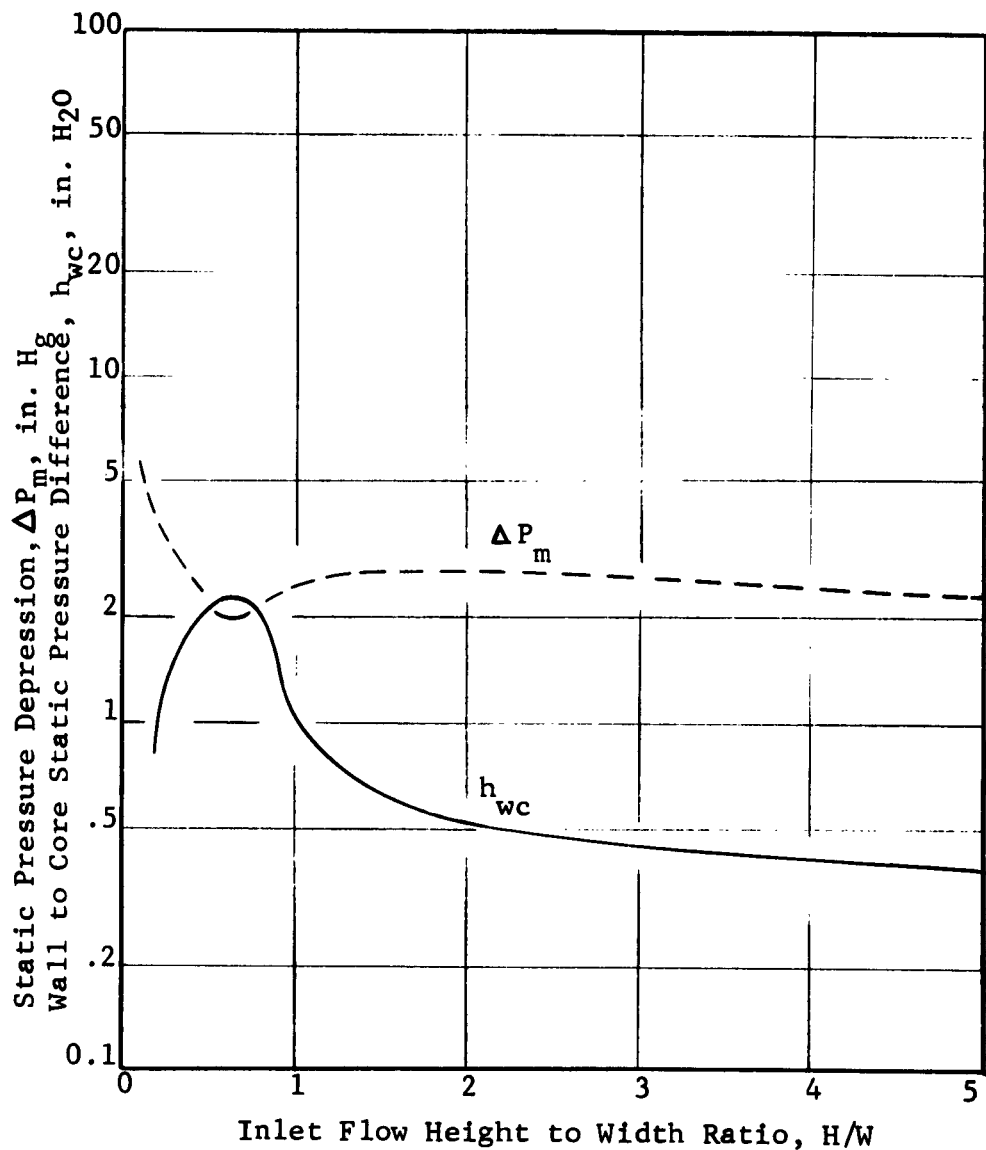


FIG. 3.4 EFFECT OF HEIGHT TO WIDTH RATIO FOR EXTERNAL INVOLUTE GENERATOR

Flow Area ( $H \times W$ ) = 2.25 sq in.

$U_o = 19.1$  fps

(See Sketch on Fig. 3.3 for  $H$  and  $W$ )

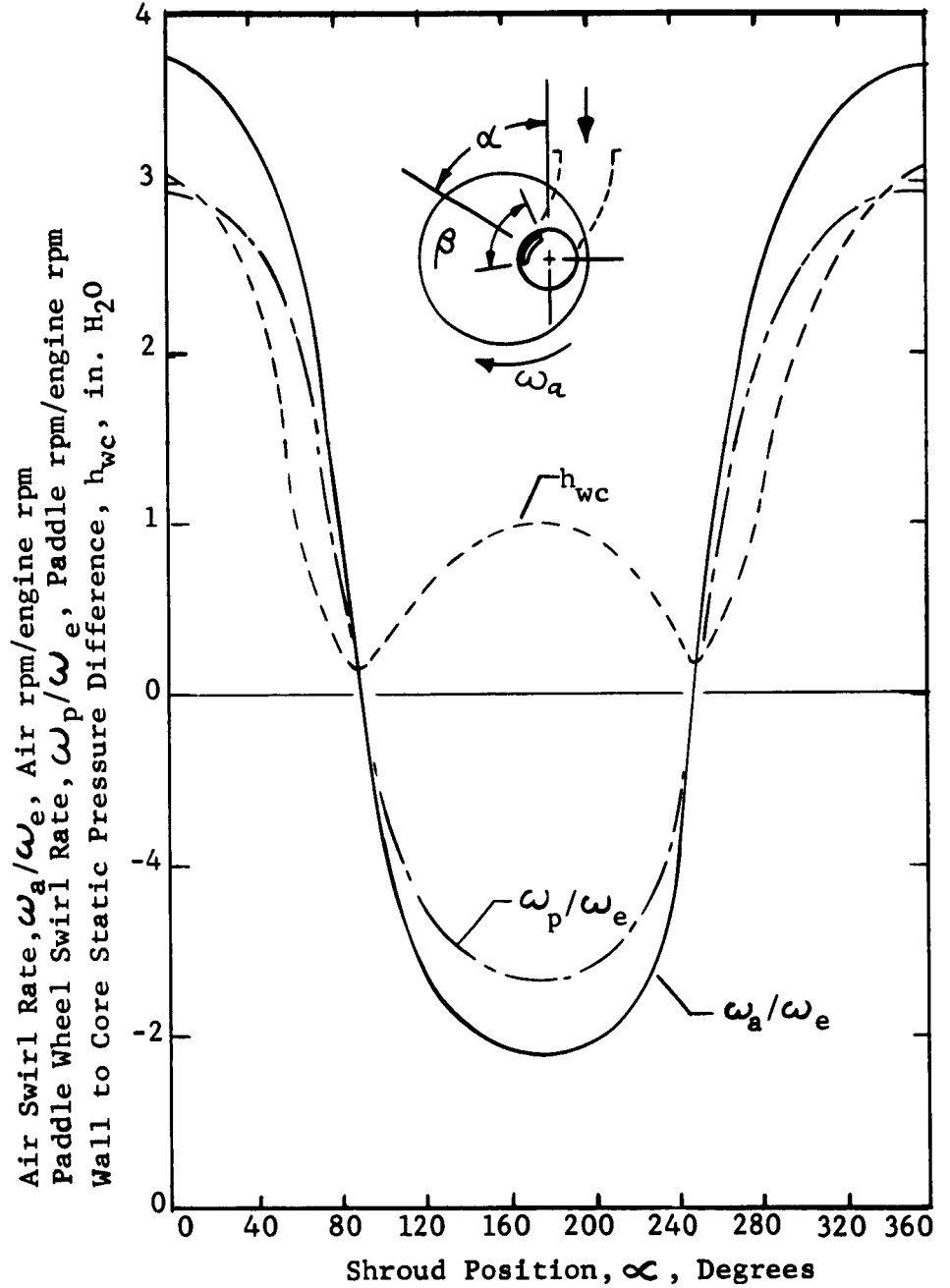


FIG. 3.5 EFFECT OF SHROUD POSITION ON AIR SWIRL

- $U = 19.1$  fps
- $z^0 = 9$  in. (from model head)
- $\beta = 100^\circ$  (shroud arc)
- $\omega_p =$  Average Speed for All Radii Tested

because of the complexities involved in moving the shroud position, still leaves much to be desired. The figure also shows the swirl rate obtained with the paddle wheel mapper. The difference in the results by the two methods comes partly from the friction in the paddle wheels and partly from the errors in the static pressure method of measuring swirl.

#### External Method

External swirl rate control should offer the advantages that the intake valve can be free to rotate, the swirl generator may be turned off to give maximum volumetric efficiency when no swirl is required, and the control mechanism can be simplified. To accomplish the variable swirl rate with the external generator, a mixing valve was inserted into the top of the generator to allow straight, nonswirling flow to mix with the tangential flow within the generator.

There was the possibility that mixing valve location above the generator might present some inflow problems. To study this a series of thin, sharp edged discs (see Fig. 2.10) with concentric holes were constructed for use as mixing valves. These were used at two locations above the generator to vary the straight flow in the top of the generator (0 and 12 inches, using a 12 inch piece of standard 2 inch pipe for the second position). The results of this test are shown in Fig.

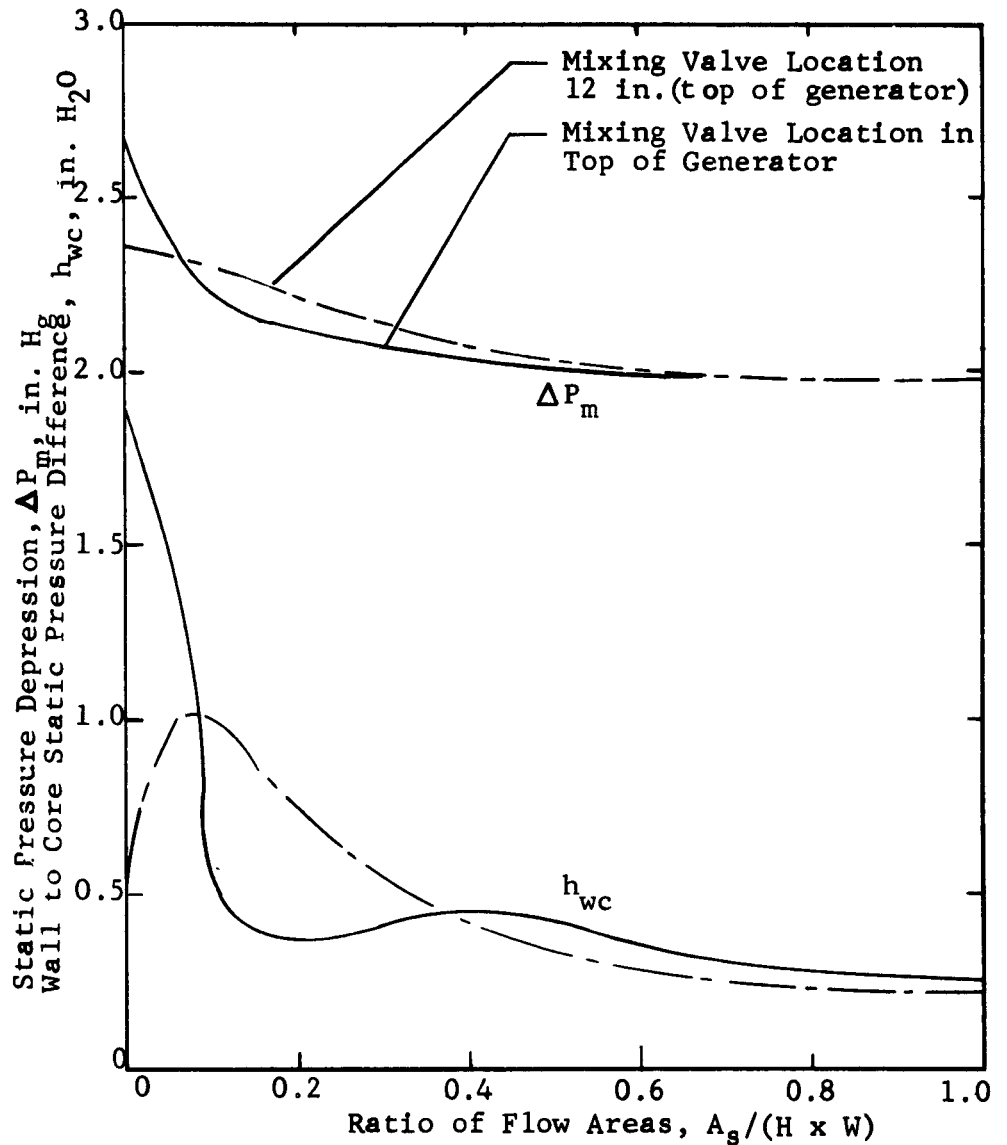


FIG. 3.6 EFFECT OF MIXING DIFFERENT PROPORTIONS OF STRAIGHT AND SWIRLING FLOWS IN THE EXTERNAL INVOLUTE GENERATOR

$U_o = 19.1$  fps  
 $A_o =$  Area of the Valve Admitting Non-Swirling Flow  
 $H = 1.25$  in.  
 $W = 1.80$  in.

3.6. These results indicated that the location of the mixing valve should be investigated further. Figure 3.7 shows the effect of mixing valve location without straight flow through the valve. For this test, sections of standard 2 inch pipe were cut off in 2 inch lengths and stacked to obtain the desired valve position. Shown in Fig. 3.8 is the static pressure distribution along the test section for two locations (0 and 4 in. above generator). It was concluded that a standing wave in the intake system destroyed the swirl with the mixing valve at the 4 inch position.

The fin generator was not investigated for variable swirl rate control characteristics because it was too difficult to install a movable fin in the present model. Such a study would have required complete redesign of the intake passage.

### 3.3 Time-Distance Relationship Studies

The most valuable result that can be gained from steady flow investigations on a model of this nature is the correlation between time and distance. With such a correlation and with the assumption that the actual intake process on the engine may be simulated under steady flow conditions, distances along the test section in the model can be related to time in the actual engine. Thus, it would be possible to predict, with some degree of accuracy, just what air flow patterns exist in the engine

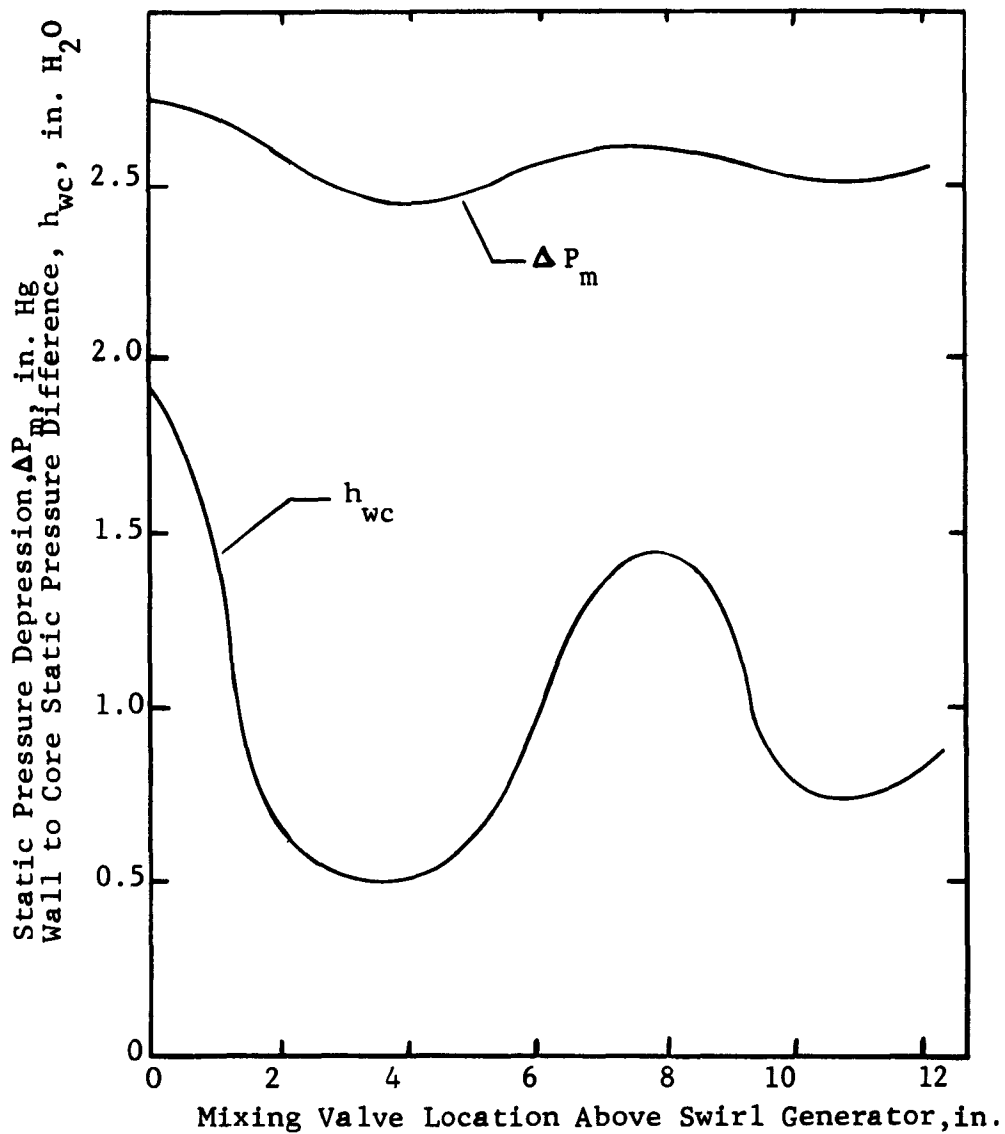


FIG. 3.7 EFFECT OF MIXING VALVE LOCATION ABOVE INVOLUTE SWIRL GENERATOR

Mixing Valve Closed (All Air Entering Through Involute Inlet)

$U_o = 19.1$  fps

$H = 1.25$  in.

$W = 1.80$  in.

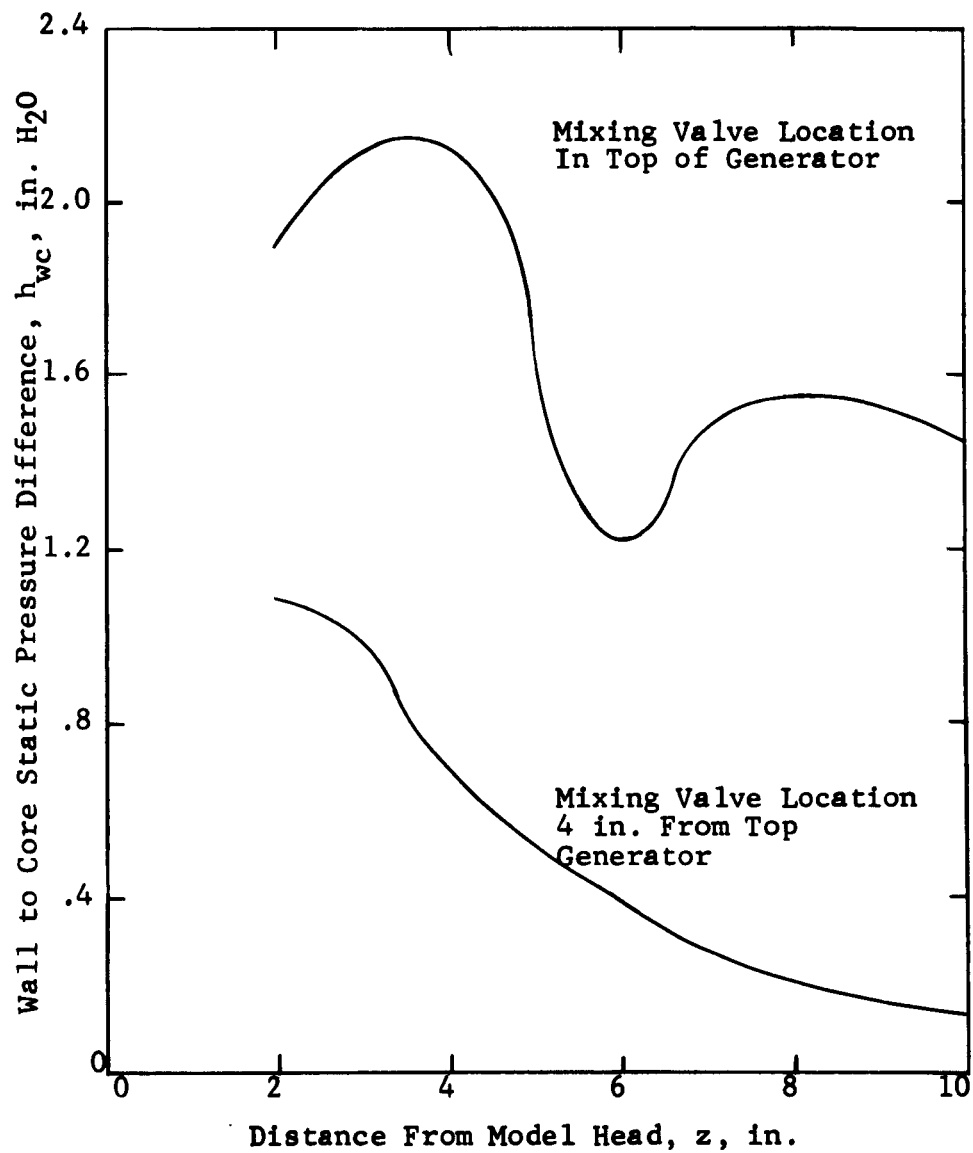


FIG. 3.8 STATIC PRESSURE DISTRIBUTION ALONG THE TEST SECTION

No Straight Flow (All Air Entering Through Involute Inlet)  
 $U_o = 19.1$  fps

at the time of fuel injection.

### Swirl Development

To investigate the time-distance relation, paddle wheel mappers (Fig. 2.6) were used to study the development of the swirl along the test section. These results showed that at small radii there was little rotation in the wake near the inlet valve but farther downstream the swirl approached a free vortex (see upper graph of Fig. 3.9). To evaluate further these tests a balsa wood paddle wheel was used (Fig. 2.6) with essentially the same results. In contrast, externally generated air swirl developed more rapidly into near solid body rotation (lower graph of Fig. 3.9). The existence of significant swirl at small radii near the inlet valve indicated that the wake air also rotated. It was concluded that this was caused by the spiraling and unimpeded outflow in all directions from the valve left area. It was also concluded that lower speed of the large radius paddle wheels at small distances from the model head was the result of added friction from a strong downwash stream caused by the incoming air flow striking the test section wall. The pressure development curves in Fig. 3.8 further substantiate this reasoning. It was concluded that the increase in the wall-to-core static pressure difference near the model head was caused, in part, by the dynamic pressure of the inflow air striking

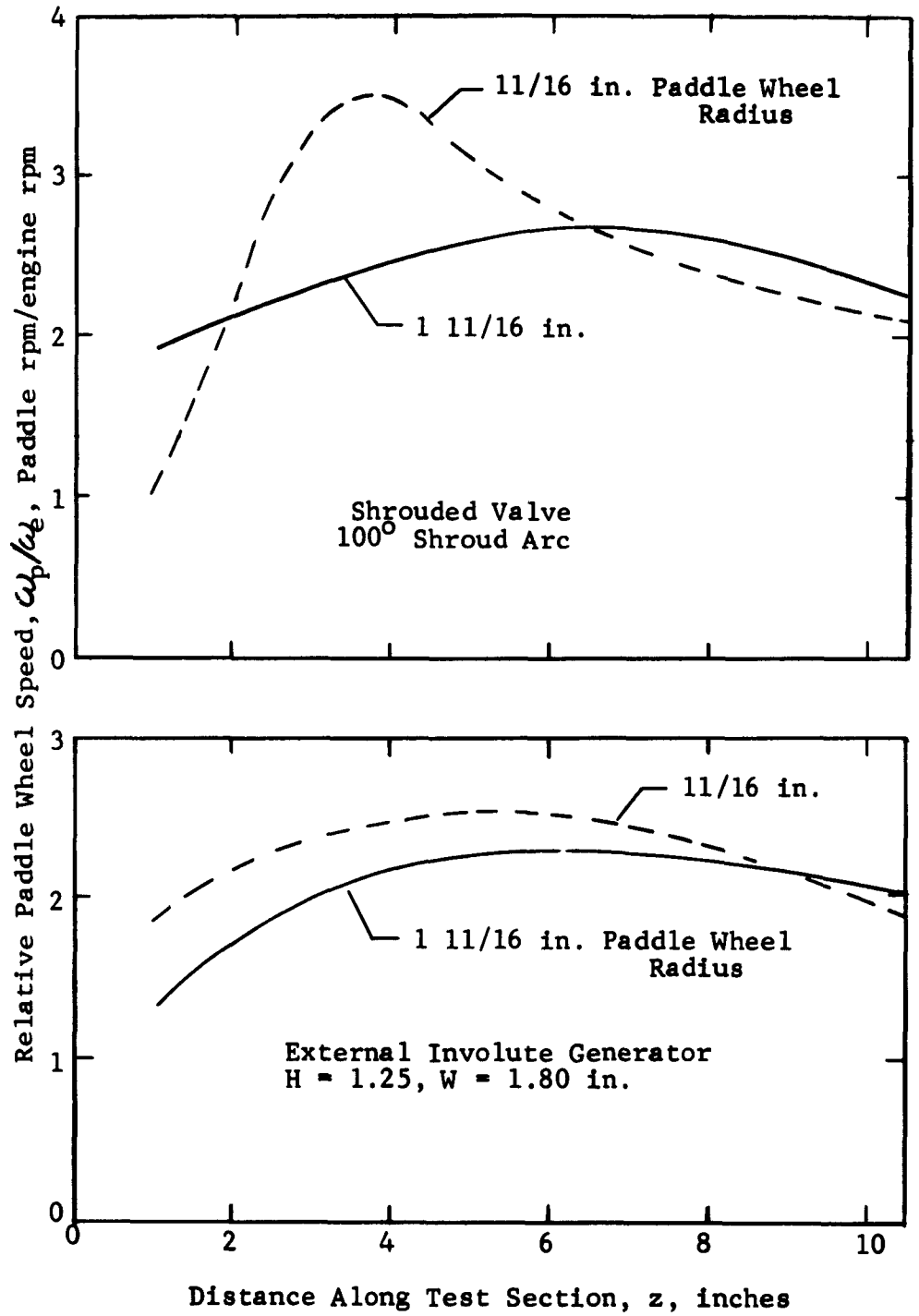


FIG. 3.9 AIR SWIRL DEVELOPMENT ALONG THE TEST SECTION.

$U_0 = 19.1$  fps

the wall.

### Transient Mapping

Shown in Fig. 2.10 are transient velocity profiles which were taken with the hot-wire network described in Section 2.5. These transient results were obtained by simultaneously closing a fast acting gate valve in the air line at the exit to the model while closing the intake valve. The two hot wires of the dual channel network were arranged so that one measured the axial velocity and the other measured peripheral velocity. Figure 3.11 shows some representative samples of the oscilloscope traces used in recording the transient velocities. Records A and B were taken at a reduced film speed to illustrate the decay process. Record C is a reproduction of a film taken at the speed that was actually used in determining the transient profiles. The higher film speed facilitated analysis. The traces on the short section of film at the right of each sample corresponds to the zero voltage signal and was used for reference. Since the hot-wire network was not linear with velocity the vertical scale is not linear but actually follows the relation given in Appendix A, Fig. B.

### 3.4 Air Swirl Symmetry

The nonsymmetry of the inflow conditions to the model suggested inquiries regarding the symmetry and

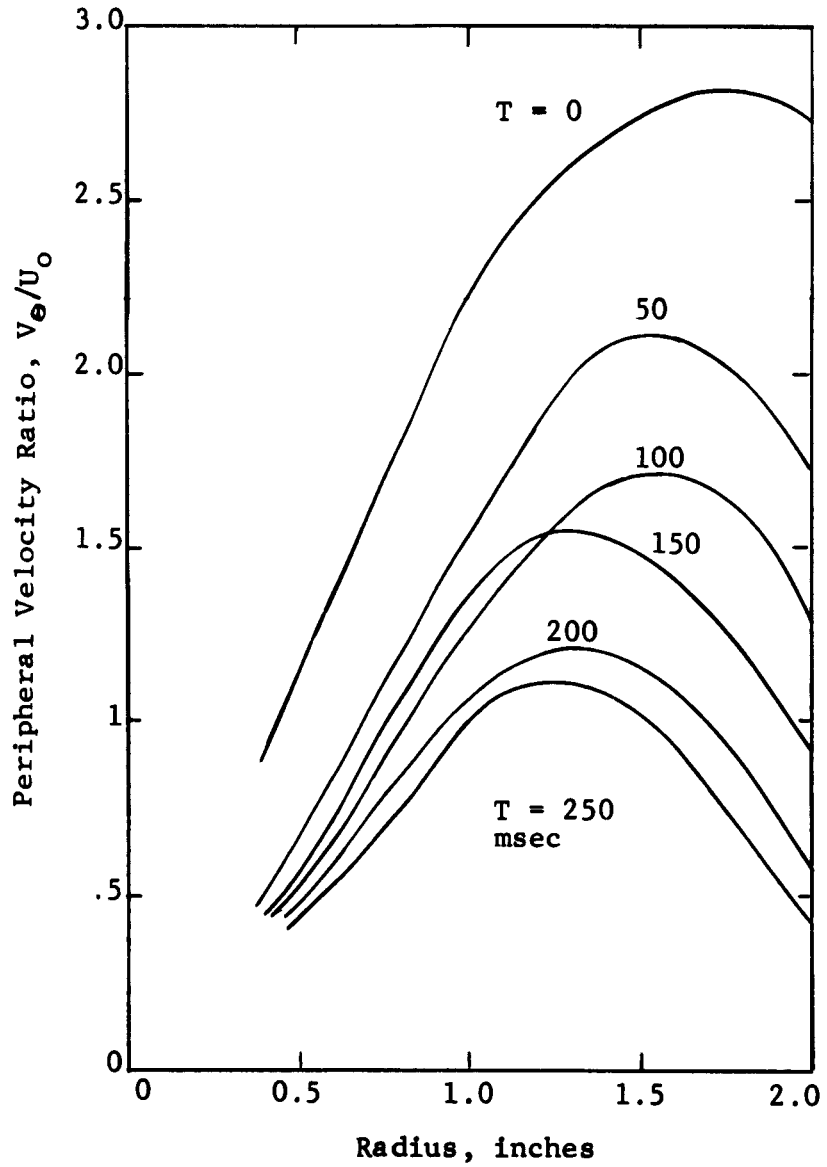


FIG. 3.10 TRANSIENT VELOCITY PROFILES

$U_0 = 19.1$  fps  
 $100^\circ$  shrouded valve  
 $z = 6$  in. (from model head)

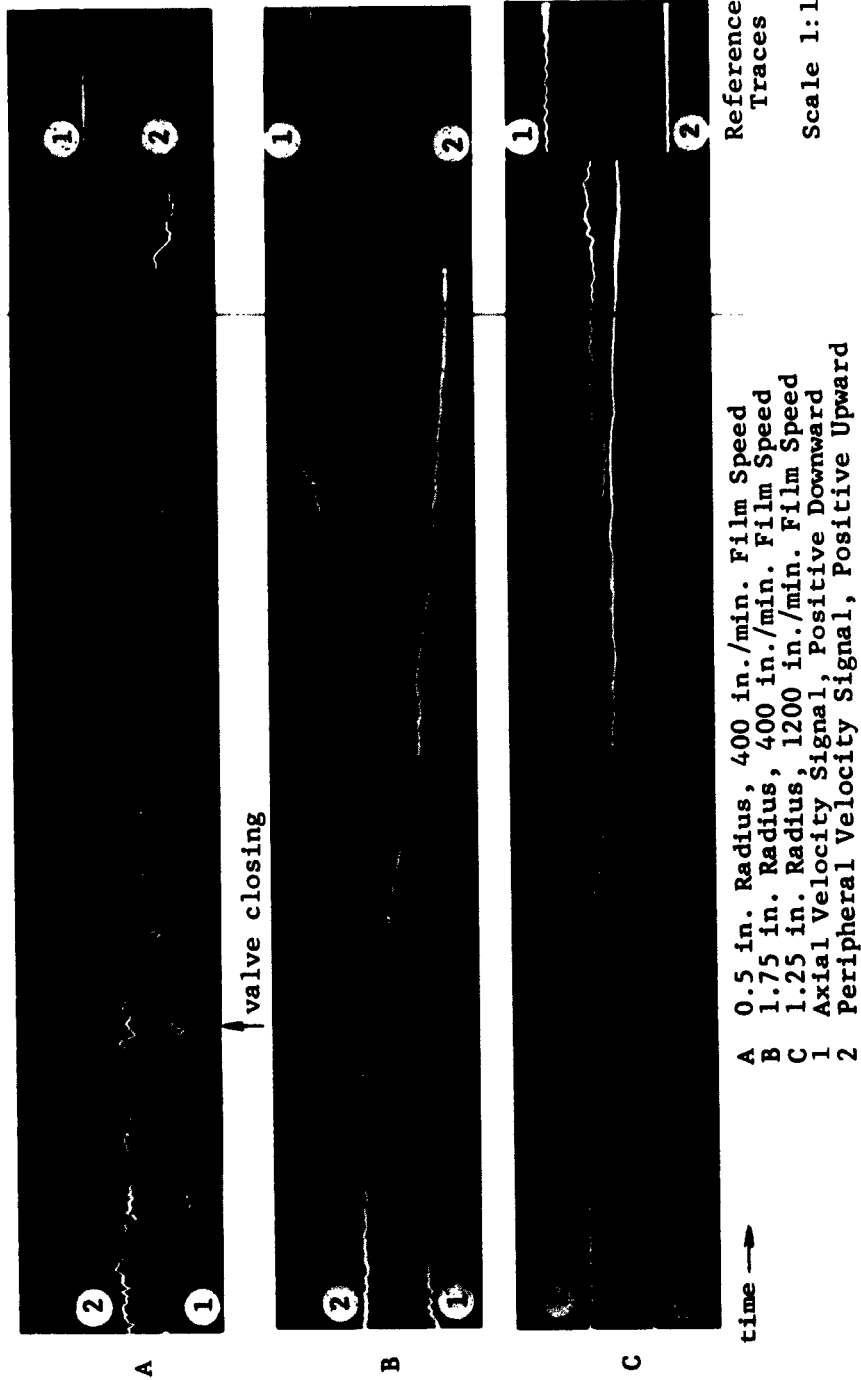


FIG. 3.11 TRANSIENT VELOCITY OSCILLOSCOPE RECORDS

shroud arc =  $100^\circ$   $U_0 = 19.1$  ft/sec  $z = 6$  in. (from model head)

instability of the developed swirl. To better understand the swirl mechanism and to evaluate further the hypothesis, velocity measurements were made at several positions around the test section. It is important from the standpoint of fuel trajectory control, that the swirl in the engine be free of cycle-to-cycle irregularities, nonsymmetry, and random behavior.

Shown in Fig. 3.12 is a polar plot of radial velocity, at a constant radius of 1 inch, for the externally generated swirl and for the shrouded valve method. These radial velocities were measured with the turbulence probe shown in Fig. 2.8 and the results were calculated by the method outlined in Appendix A. Figure 3.12 indicates that the shrouded valve produces an offset swirl (which would be felt in the engine as core motion) while the external generated swirl produced a relatively symmetrical swirl. It should be noted also that the radial velocity plot for the externally generated swirl shows a net flow inward toward the geometric center. This inward flow, it was assumed, was induced by the low pressure wake near the inlet valve. Figure 3.13 shows some results of flow direction azimuth measurements by the method described in Section 2.3. These azimuth results, in conjunction with the variations in peripheral and axial velocities around the test section (Fig. 3.14), further demonstrate the flow nonsymmetry that existed in

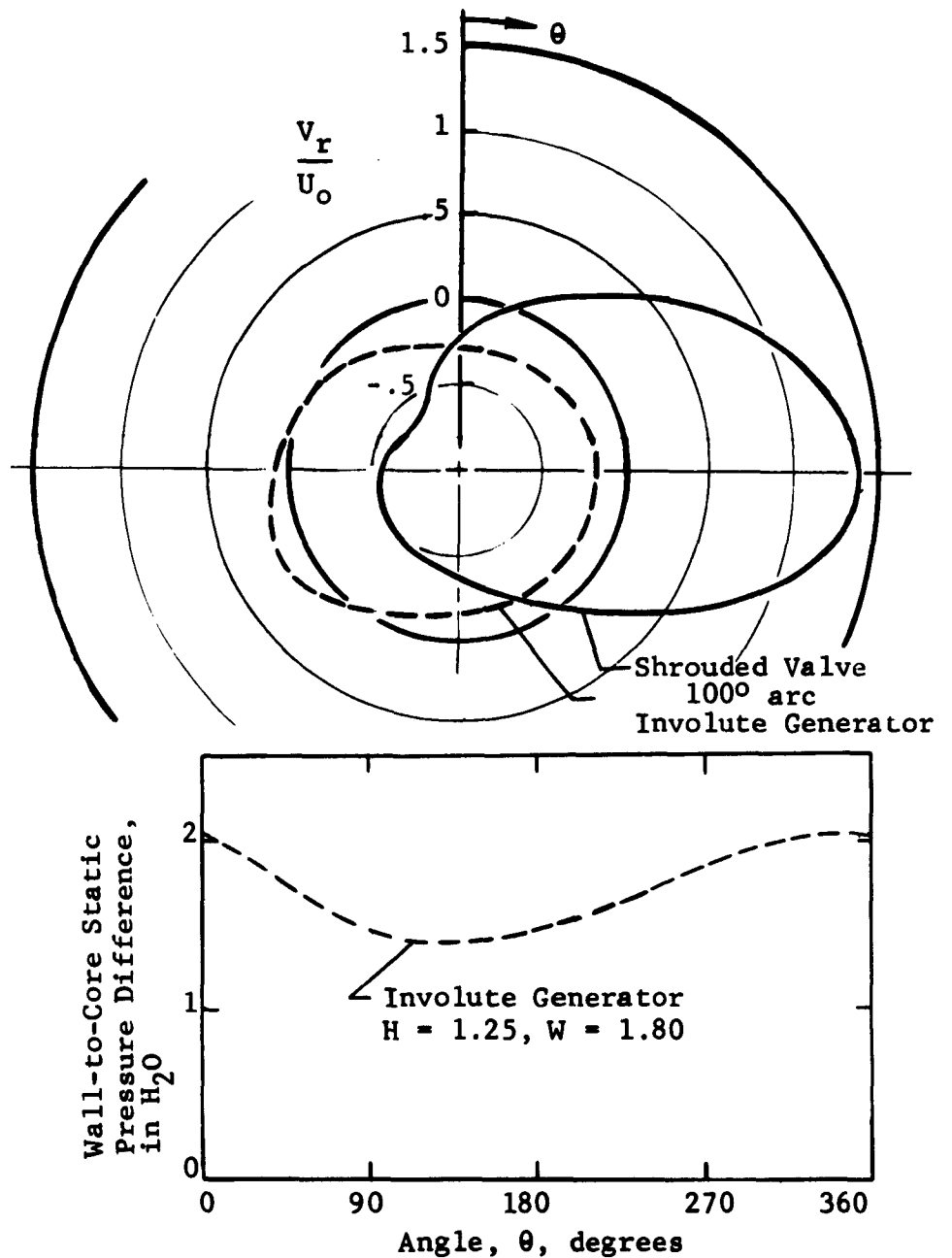


FIG. 3.12 RADIAL VELOCITY FLUX AT 1 INCH RADIUS AND STATIC PRESSURE DISTRIBUTION AROUND THE TEST SECTION

$z = 9$  in. (from model head)

$U_o = 19.1$  fps

$\theta$  is measured clockwise viewed from downstream direction

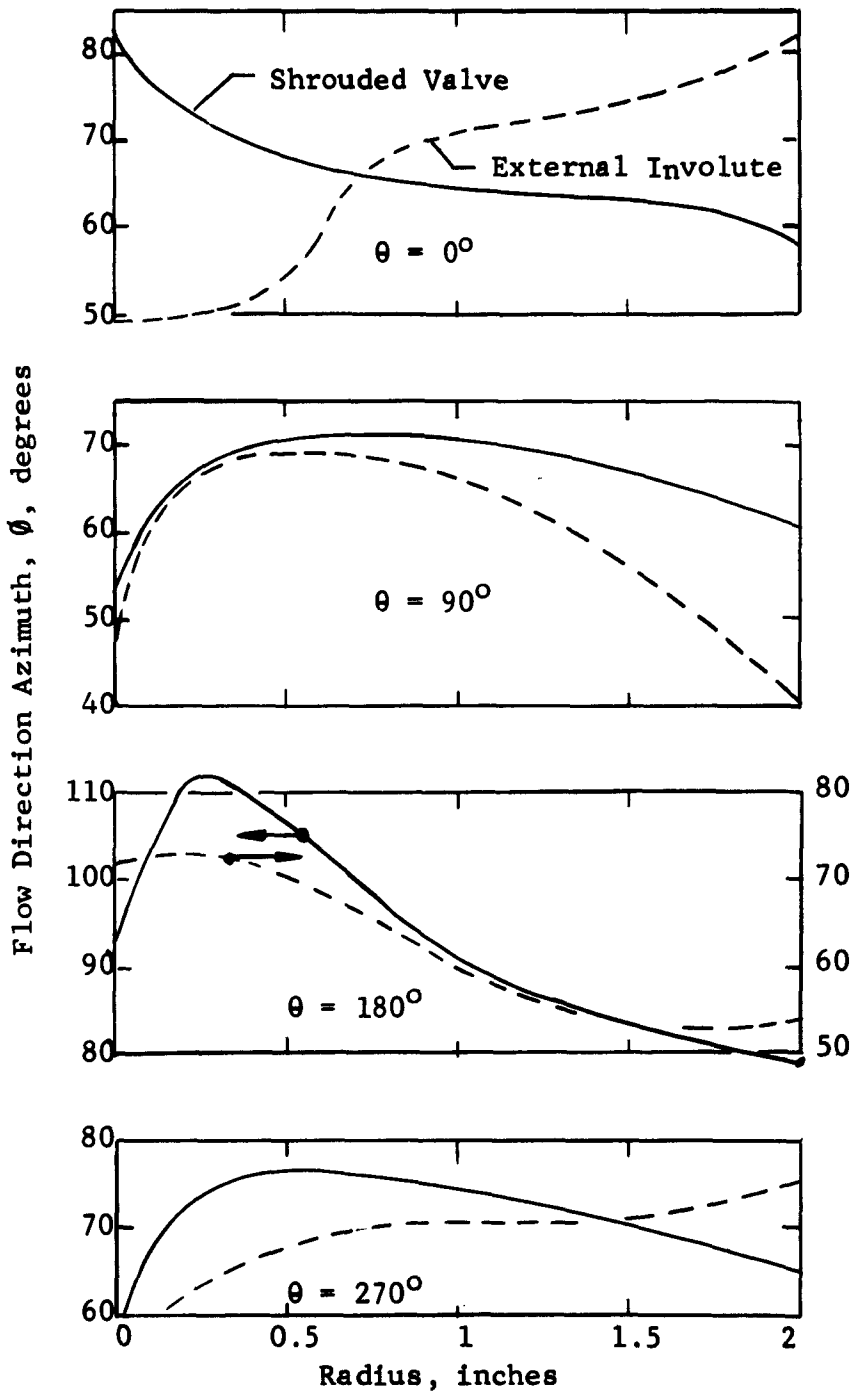


FIG. 3.13 EFFECT OF UNSYMMETRY ON FLOW DIRECTION AZIMUTH  
 flow conditions same as for Fig. 3.12

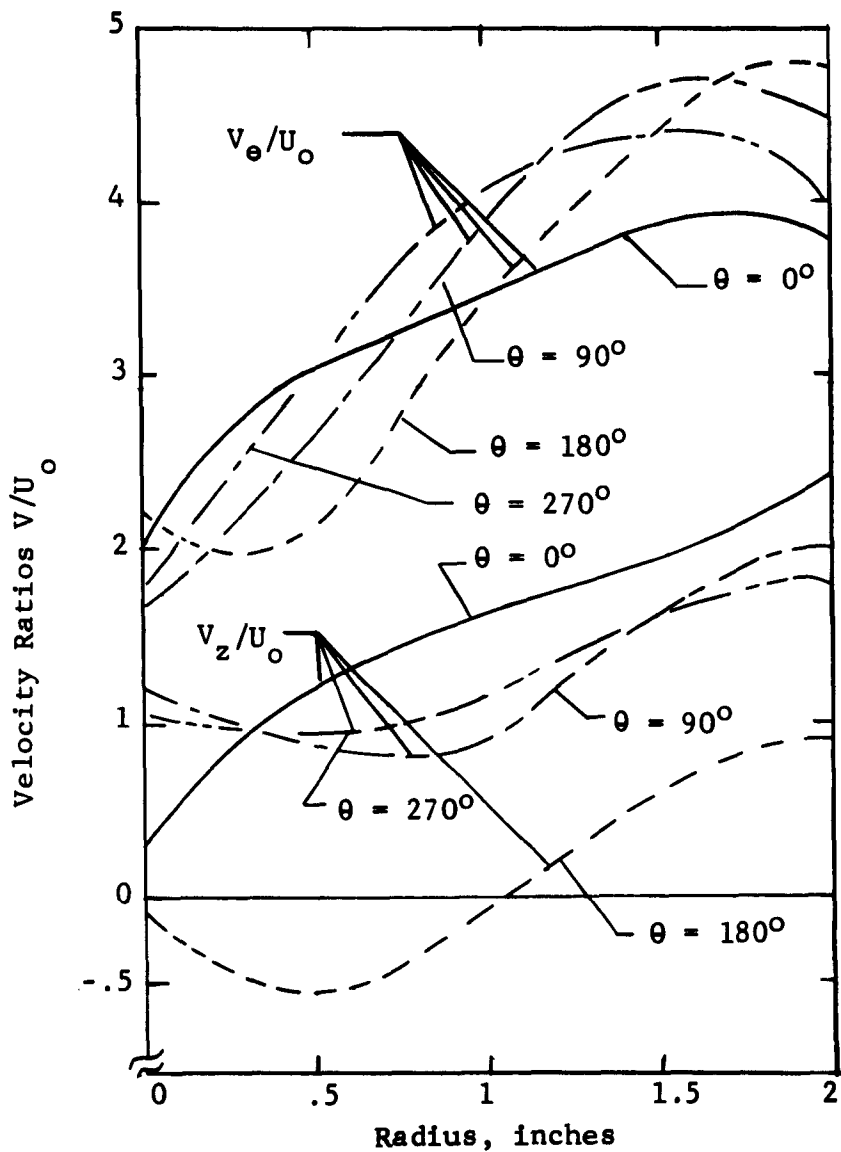


FIG. 3.14 EFFECT OF UNSYMMETRY OF FLOW ON PERIPHERAL AND AXIAL VELOCITIES

shroud arc =  $100^\circ$   
 $U_0 = 19.1$  fps  
 $z = 9$  in.  
 $V_\theta$  = Peripheral Velocity  
 $V_z$  = Axial Velocity

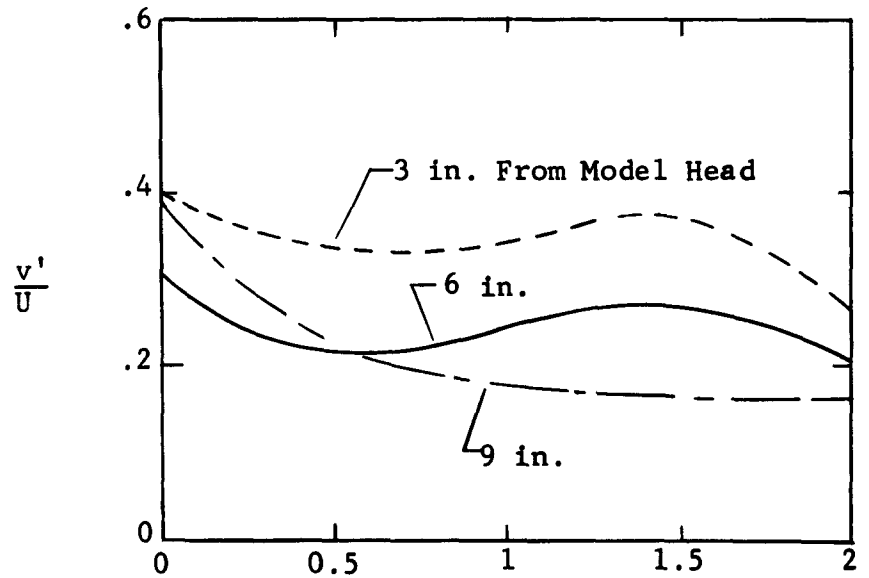
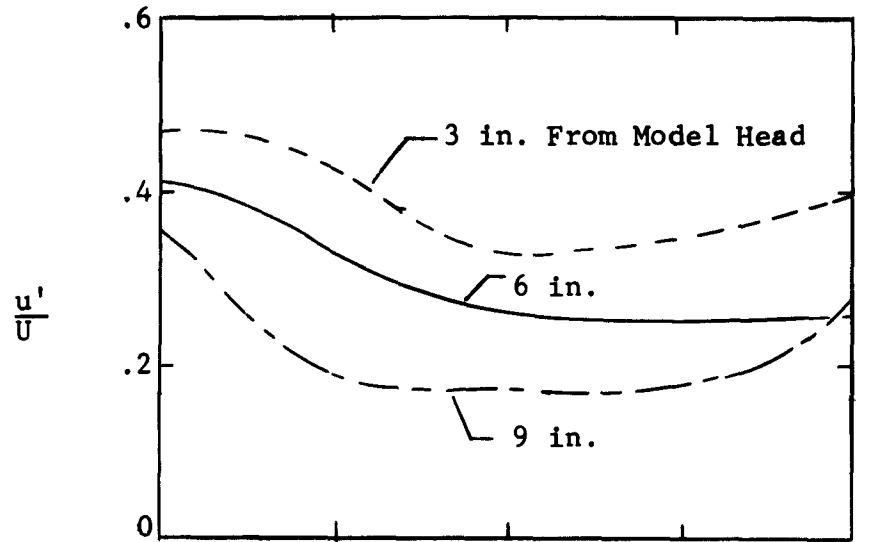
the model.

The presence of the probe itself introduced large relative errors in the azimuth measurements at small radii hence the axial velocity measurements did not coincide at the geometric center. For purposes of comparison it was necessary to map the velocities at eight different angular locations ( $\theta$ ). The results were then averaged to indicate a mean swirl rate and are shown in Fig. 3.15.

### 3.5 Turbulence Measurements

In homogeneous charge engines and in Diesel engines the existence of a high level of turbulence in an important aid to evaporation and combustion of the fuel. Mechanisms such as squish are often provided to produce turbulence. In the spark ignited, stratified charge engine turbulence might diffuse the fuel spray too rapidly. Turbulence was, therefore, mapped by the method described in Section 2.4 to compare the different swirl producing methods.

The turbulence probe used in this investigation could measure turbulent intensities only in the radial and mean flow directions. Figure 3.16 shows the turbulent intensities at different locations in the test section for the 100<sup>o</sup> shrouded valve. The rms (root mean square) variation ( $u'$ ) of the mean flow ( $U$ , in the tangential direction) is shown to decrease with distance



Radius, inches

U is the mean velocity in the flow direction

$u'$  is the RMS variation of U

$v'$  is the RMS variation transverse to U

FIG. 3.16 TURBULENT INTENSITIES FOR SHROUDED VALVE GENERATED AIR SWIRL

shroud arc = 100°

$U_0 = 19.1$  fps

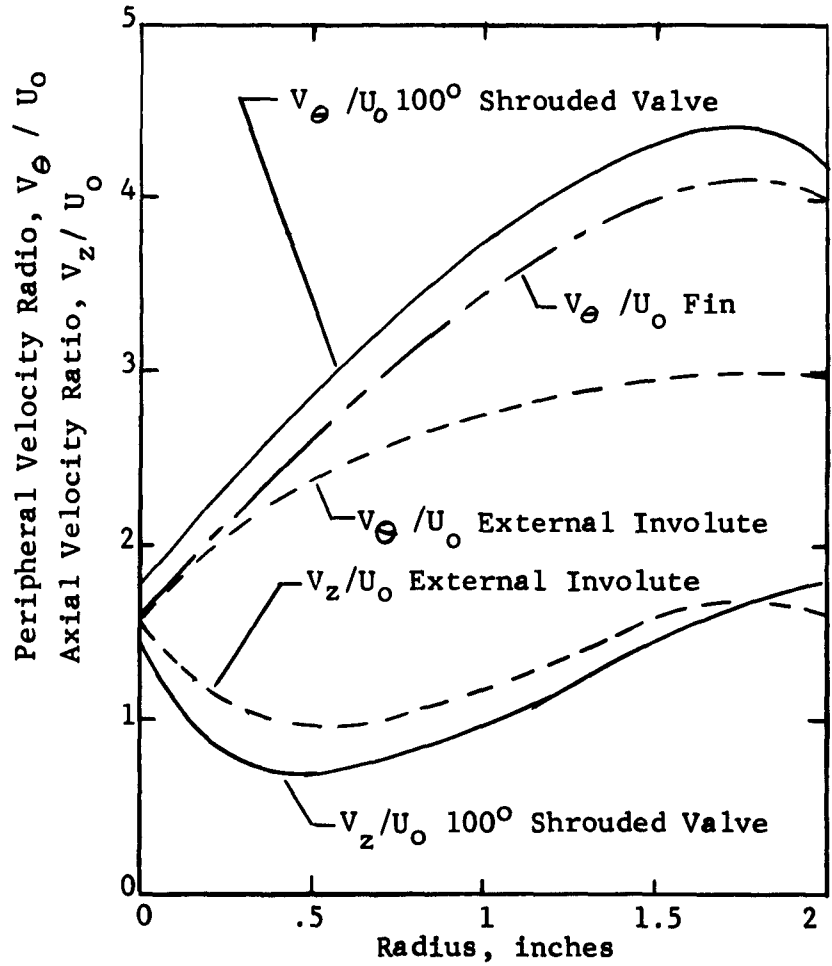
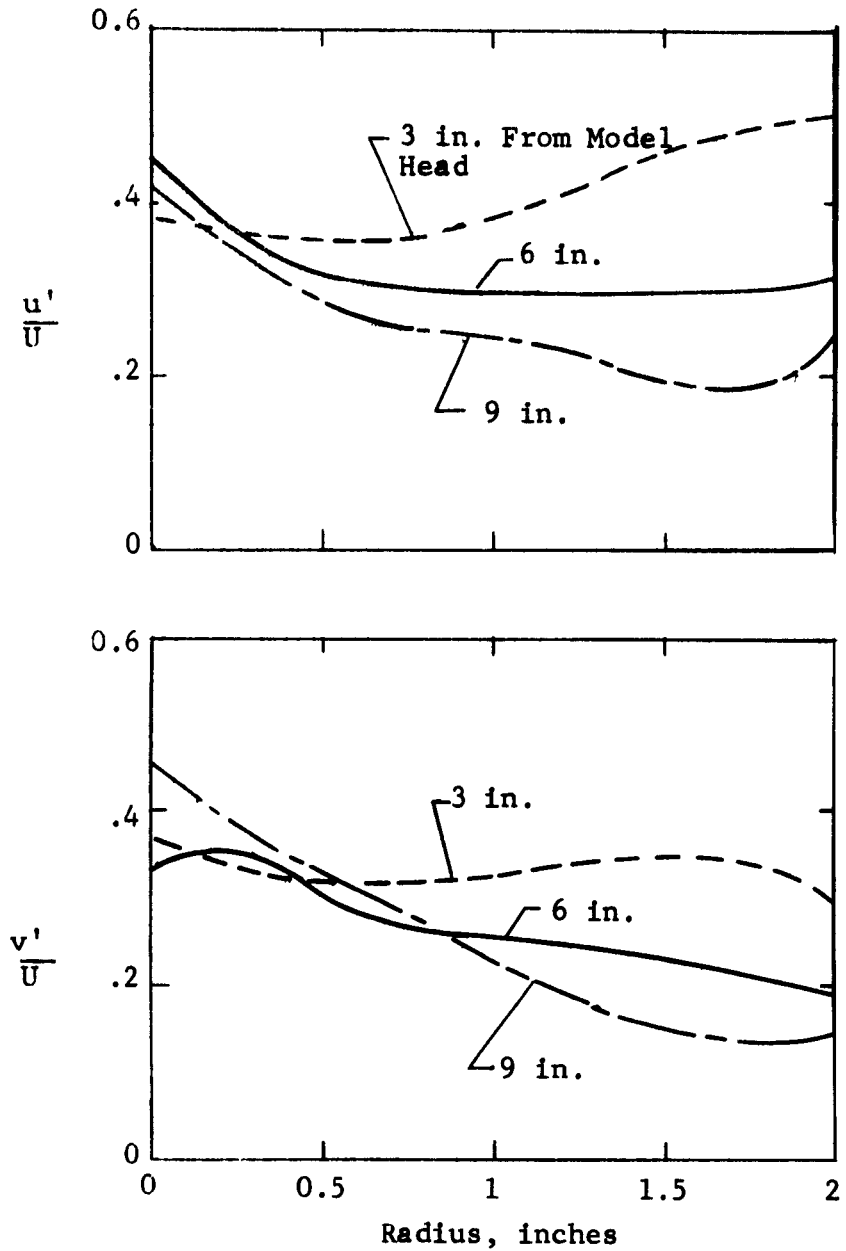


FIG. 3.15 AVERAGED MEAN FLOW VELOCITIES

$z = 9$  in. (from model head)  
 $U_0 = 19.1$  fps

from the model head. A similar decrease is shown to occur for the transverse velocity fluctuations ( $v'$  in the radial direction). The figure shows a definite increase in turbulence at small radii which was caused in part by the presence of the probe and in part by the nature of the core pressure gradients. The general decrease of the turbulent intensities along the test section further substantiates the possibility of time-distance transformations. Similar results for the external involute generator are shown in Fig. 3.17.

A comparison of the turbulent intensities in the swirls produced by the different generation methods (including the fin) is shown in Fig. 3.18. These results (Fig. 3.18) indicate that the fin generator produced a noticeably lower level of turbulence than the other generators while still producing a high swirl rate (Fig. 3.15).



$u'$ ,  $v'$ , and  $U$  are defined in Fig. 3.16

FIG. 3.17 TURBULENT INTENSITIES FOR THE EXTERNAL INVOLUTE GENERATED AIR SWIRL

$$U_0 = 19.1 \text{ fps}$$

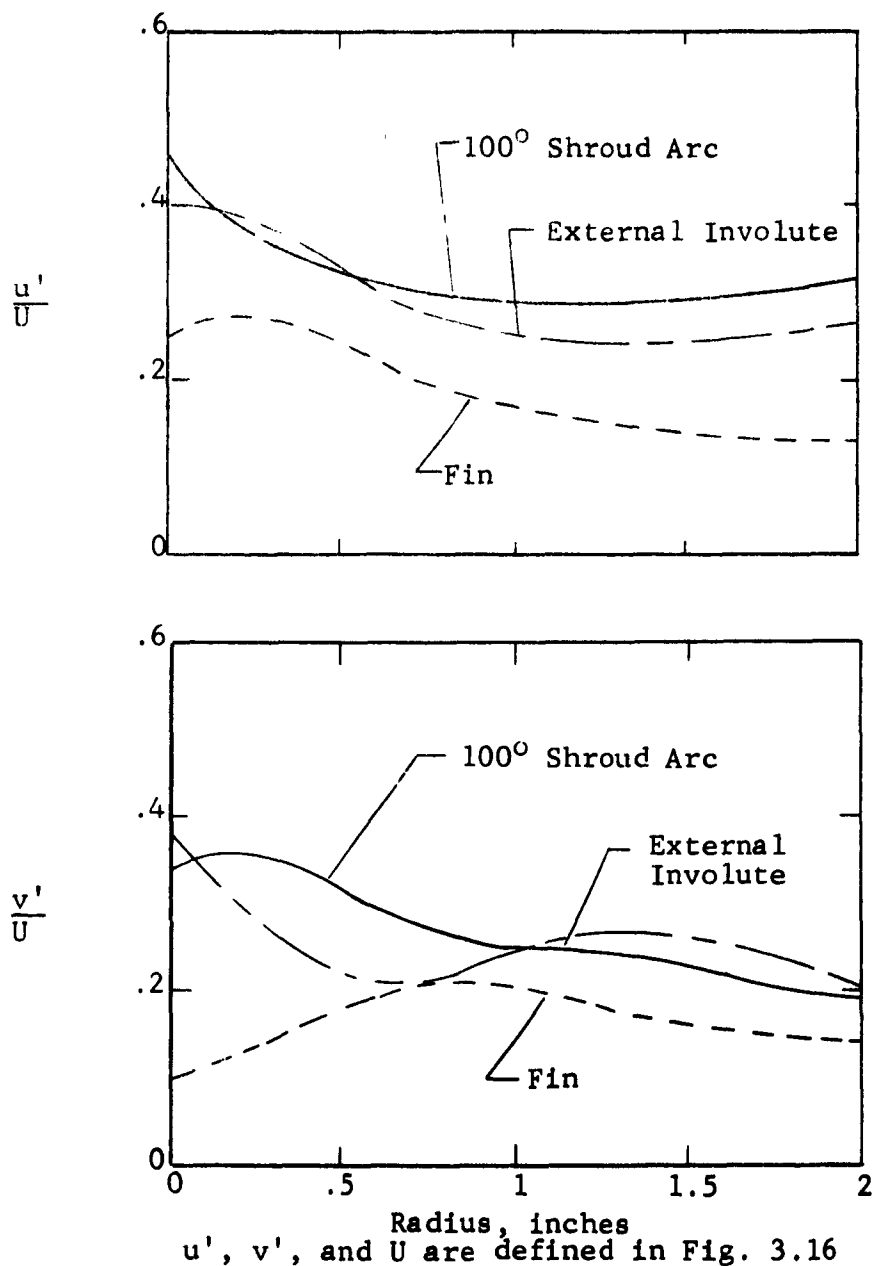


FIG. 3.18 COMPARISON OF TURBULENT INTENSITIES

$z = 6$  in. (from model head)  
 $U_0 = 19.1$  fps

#### IV. ANALYSIS OF RESULTS AND HYPOTHESES

##### 4.1 Analysis of Results

The results are best compared by considering different forms of the vorticity equation. These can be derived from the momentum equation in tensor form

$$\frac{D u_i}{D t} = f_i - \frac{1}{\rho} \frac{\partial P}{\partial x_i} + \frac{1}{\rho} \frac{\partial}{\partial x_j} T_{ij}^{(v)} \quad (1)$$

where  $u_i$  is the particle velocity in the  $i$  direction,  $f_i$  is the body force,  $T_{ij}^{(v)}$  is the viscous shear stress tensor, and  $D/Dt$  is the substantial material derivative.

The above velocity term in Lagrange formulation can be related to the Euler formulation as follows

$$\frac{D u_i}{D t} = \frac{\partial u_i}{\partial t} - e_{ijk} u_j \Omega_k + \frac{\partial}{\partial x_i} \left( \frac{u_k u_k}{2} \right) \quad (2)$$

where  $e_{ijk}$  is the permutation tensor, and  $\Omega_k$  is the vorticity.

Upon substitution of the acceleration from Equation 2 into Equation 1 and taking the curl ( $e_{imn} \partial / \partial x_m$ ) of the resulting equation the following form is derived

$$\begin{aligned} \frac{D}{D t} \left( \frac{\Omega_m}{\rho} \right) &= \frac{\Omega_k}{\rho} \frac{\partial u_m}{\partial x_k} \\ &+ \frac{e_{lmn}}{\rho} \frac{\partial}{\partial x_i} \left( f_i - \frac{1}{\rho} \frac{\partial P}{\partial x_i} + \frac{1}{\rho} \frac{\partial}{\partial x_j} T_{ij}^{(v)} \right) \quad (3) \end{aligned}$$

This equation, according to Serrin (21), governs the convection vorticity and is called the vorticity equation.

This same result derived by considering the circulation around a fluid element is discussed by Lamb (22).

By assuming only conservative body forces (i.e.,  $f_i \propto u_i$ ) the body force term is zero because the curl of the gradient ( $u_i$ ) is zero. By also assuming adiabatic flow ( $\rho = c p^{1/k}$ ) the term containing the pressure gradient also vanishes and the resulting equation is

$$\frac{D}{Dt} \left( \frac{\Omega_m}{\rho} \right) = \frac{\Omega_k}{\rho} \frac{\partial u_m}{\partial x_k} + e_{lmn} \frac{\partial}{\partial x_i} \left( \frac{1}{\rho} \frac{\partial}{\partial x_j} T_{ij}^{(v)} \right) \quad (4)$$

This equation will be used to describe the energies involved in various swirl generation methods.

#### Effect of Viscosity

The analysis can best be made with the following considerations:

- (1) Assume the density ( $\rho$ ) to be constant, except across the intake valve restriction.
- (2) Assume the viscosity ( $\mu$ ) to be constant throughout.

With these assumptions the vorticity equation (Eq. 4) reduces to

$$\frac{D}{Dt} (\Omega_m) = \Omega_k \frac{\partial u_m}{\partial x_k} + \nu \frac{\partial^2}{\partial x_j^2} (\Omega_m) \quad (5)$$

where  $\nu$  is the kinematic viscosity, the first term is the production of vorticity by stretching, and the second term is the dissipation of vorticity by viscosity.

In the case of the external can generator the

vorticity ( $\Omega_k$ ) was generated in the can and accelerated by intake size reduction ( $\partial u_m / \partial x_k$ ). During this process energy was dissipated by viscosity.

For the case of the involute generator, stretching did not occur but it was still necessary to turn the swirl (vortex) around a  $90^\circ$  corner. If  $\Omega_m$  is now taken as the vorticity in the z direction (along the cylinder axis) Equation 5 shows that there is no justification for swirl to exist in that direction, because  $\Omega_k$  was generated at right angles to the cylinder axis. The test results indicated that for some external generator configurations little or no swirl reached the cylinder. It was concluded that the swirl that was generated with the "optimum" configuration of the external involute generator came from the viscous forces involved in dissipating the  $\Omega_k$  vortex.

To examine further the problem of turning the vortex and its destruction in the intake passage, a Hewlett-Packard 302-A Wave Analyzer was connected to the output of an audio microphone for the purpose of studying the pulsating noise in the intake. The results indicated that the optimum involute generator produced a 505 cps pulsation with a rather large amplitude. When the mixing valve (closed) was moved to the 4 inch position (see Figs. 3.7 and 2.10) the pulsations were at 430 cps and their amplitude was greatly reduced. Both the frequency and

amplitude of the pulsations increased as the mixing valve was moved to the 8 inch position indicating the return of the disturbance. Calculations showed the frequency to be that of harmonic pipe tuning at the prevailing flow velocities. It was not determined whether the tuning effect prevented swirl development or lead to swirl destruction. It was concluded, however, that the intake pipe tuning greatly affected the external generation.

#### 4.2 Analysis of the Hypothesis

The "swirl induced" stratified charge system, as discussed before, is a process in which fuel is localized near the centrally located spark plug by the interaction of the injected fuel spray with the air motion in a cylindrical chamber. This process to be efficient requires an air swirl that is symmetrical about the chamber axis and free from gross transverse motion that would tend to disturb the fuel spray pattern.

##### Hypothesis:

It is believed that an externally generated swirl would flow in through the intake valve in an organized manner such that little turbulence in the upper portion of the chamber would result thus providing a clean swirl. On the other hand, the shrouded or masked intake valve provides inflow in all directions from the unmasked area thus very likely causing turbulence and random motion in the upper portion of the cylinder.

The plot of radial velocity flux (Fig. 3.12) demonstrates

that this hypothesis was found to be valid. Figure 4.1 shows the flow patterns that were found to exist in the flow model. Shown also in Fig. 4.1 is a graphical description of the swirling flows believed to exist in the engine at the time of injection and during the subsequent compression stroke.

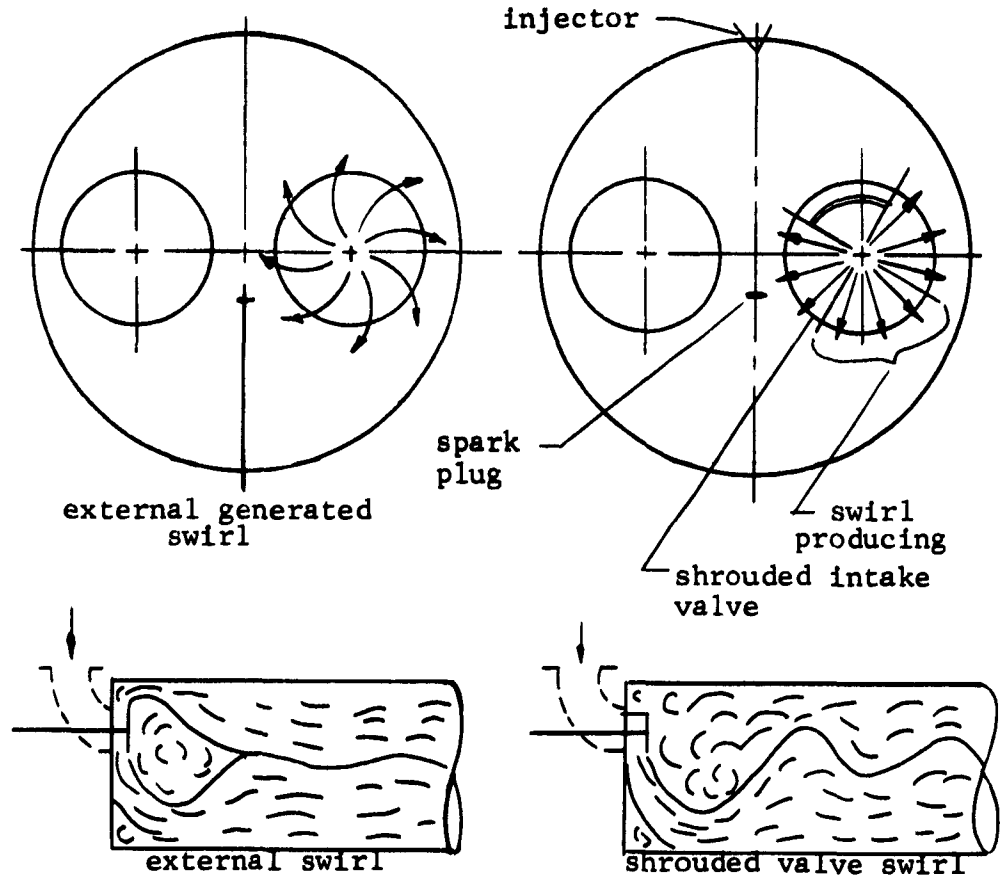
As part of the program the swirl rate was evaluated by measuring the wall-to-core static pressure difference. Under most conditions this pressure difference would vary slightly with time, indicating instability and unsymmetry of the generated air swirl. This did not occur with the fin generator and, therefore, it was concluded that it produced a stable and symmetrical swirl with a stationary core axis.

#### 4.3 Engine Considerations

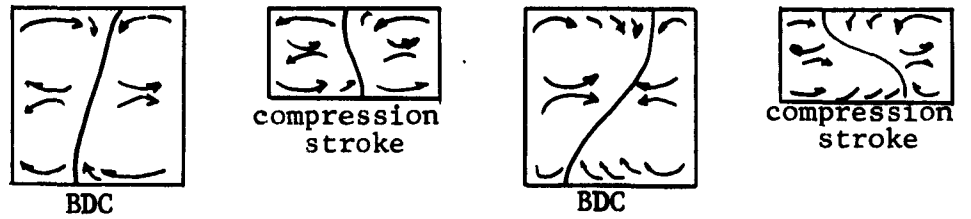
The ability to relate the air motion in the model and to that in the actual engine is the one most important factor justifying steady flow model studies. With such a relationship established, the simple measurements in the model provide insight into the very complicated transient, swirl generation process in the engine.

There were several considerations in relating model and engine:

- (1) The production of similar swirl rates at the same integrated flows in the model and in the engine.



Observed Flow Patterns



Engine Swirl Patterns

FIG. 4.1 DESCRIPTION OF HYPOTHESIZED AND OBSERVED FLOW

- (2) The relation between distance in the model and time in the engine.
- (3) The extension of the investigation of intake induced flow patterns into the compression stroke.

Using the assumption of similar flows in engine and model at equal integrated flows a procedure for estimating air swirl rate was derived. It is given in Appendix D. The result of this simple study showed that the swirl rate is not a function of engine speed. Measurements by Ricardo (8) and others in actual engine cylinders showed this to be true at least over a limited range of engine speeds.

For example, a swirl rate of 3.75 was calculated by the method of Appendix D for 80% volumetric efficiency and  $90^\circ$  shroud arc. Measurements on the model (Fig. 3.1) indicated that a  $90^\circ$  shroud arc produces a swirl rate of 3.50. These results also compare quite well with those reported by Ricardo for similar conditions.

The mechanism of intake induced swirl generation is best described as follows: The swirl, when first generated, tends toward free vortex rotation because the incoming air is basically irrotational and in accordance with Kelvin's theorem of minimum energy (22) a free vortex contains the lowest possible energy level. At this point the air viscosity and the high shear rates of

free vortex flow introduce a high level of turbulence. Because the turbulence shear stresses (momentum transfer stress) are so large compared to the laminar shear stresses existing at the chamber walls (only laminar flow can exist at a solid boundary) the swirl immediately changes to near solid body rotation. This rotation continues on, into the decay process, until the free-stream turbulent stresses are of the same order of magnitude as the laminar wall stresses. These wall stresses introduce a shift of the peak peripheral velocity toward the chamber center. The vorticity decay by viscosity process is described in detail by Schlichting (23).

Figure 3.8 shows that the shrouded valve generated swirl in this manner, while the externally generated swirl confined the free vortex rotation to the intake passage. This compares very well with Lee's (10) reported results of swirl mapping in an engine cylinder. (The development along the test section of the fin generated air swirl was not investigated.)

The shift in the transient decay curve is shown in Fig. 3.10. It should be noted also that the rate of decay is quite slow. This is best shown by an example. At the engine speed associated with the flow model test of Fig. 3.10 (1900 rpm) 55 milliseconds will elapse from the end of one intake stroke to the beginning of the

next. The transient tests on the model indicate approximately a 25% reduction in swirl during that same period; hence the clearance gases will probably still contain significant swirl.

A direct transformation of model velocities with distance to the engine velocities with time would be possible ( $t = z/V_z$ ) if the axial velocity did not vary significantly across the test section. Figure 3.15 shows that for the shrouded valve and fin generator the swirling peripheral velocity was quite high compared to the axial velocity and that the latter deviated somewhat from the average. Figure 3.16 shows a general reduction in turbulence along the test section which demonstrates the time decay process.

Similar results for the involute generator (Fig. 3.17) did not show any significant change in the turbulence level for external swirl generation. This was due mainly to the turbulence generated in turning the swirl around the corner of the intake passage.

When the swirl was generated in the intake passage in the direction of the cylinder axis the turbulence was reduced (shown by the comparison of Fig. 3.18). This reduction has three causes:

- (1) The vorticity from turning the corner in the intake passage was simply converted into a swirl along the cylinder axis.

(2) The swirl was generated farther upstream and therefore the turbulence had a longer time to decay.

(3) The inflow velocities were reduced because the full valve lift area was used.

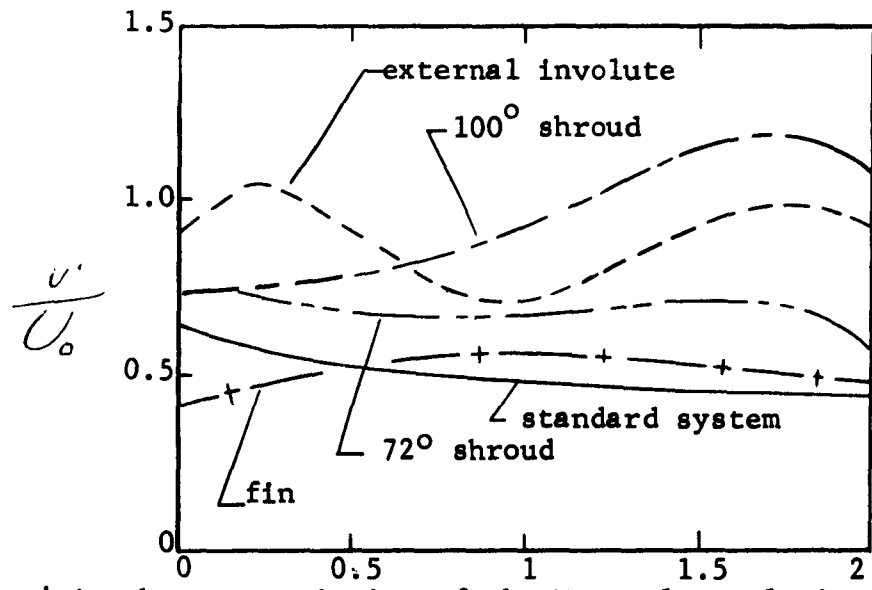
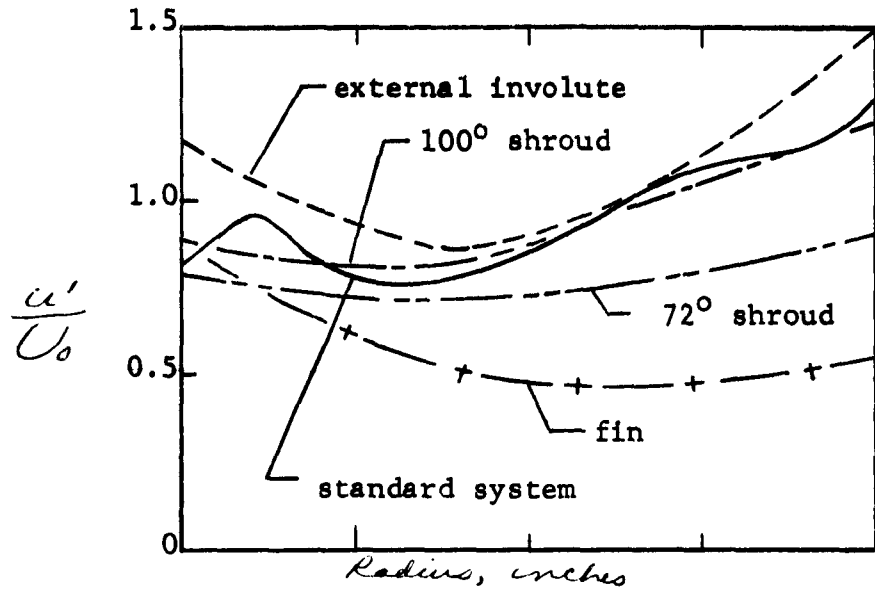
The relative turbulent intensities are further compared in Fig. 4.2. These results show that the fin generator provided a clean air swirl with a turbulence level as low or lower than the standard intake system.

It was concluded that the fin method of swirl generation would be best from the standpoint of stratification of an injected fuel spray. It should be noted also that the level of turbulence in the actual engine would be somewhat lower than those measured in the model because the full valve lift would be used, thus reducing the turbulence.

#### Compression of Vorticity

By considering the air trapped in the engine cylinder as a perfect fluid ( $\mu = \text{const.}$ ) adiabatic, and in a conservative force field, the air motion during the compression stroke can be analyzed readily. With these assumptions, Equation 3 reduces to

$$\frac{D}{Dt} \left( \frac{\Omega_m}{\rho} \right) = \frac{\Omega_k}{\rho} \frac{\partial u_m}{\partial x_k} \quad (6)$$



$u'$  is the rms Variation of the Mean Flow Velocity  
 $v'$  is the rms Variation Transverse to  $u'$   
 $U_0$  is the Average Axial Flow Velocity

FIG. 4.2 COMPARISON OF PERTURBATION VELOCITIES

$U_0 = 19.1$  fps  
 $z_0 = 6$  in. (from model head)

This is integrated by Serrin (23) to give Cauchy's equation

$$\frac{\omega_i}{\rho} = \frac{\omega_m}{\rho_0} \frac{\partial X_i}{\partial a_m} \quad (7)$$

where  $\omega_i/\rho$  is the instantaneous vorticity at any time, and  $\omega_m/\rho_0$  is the initial vorticity.

Consider now a material line element (length,  $dx_m$ ) in the direction of the initial vorticity ( $\omega_m/\rho_0$ ) to be proportional to that vorticity, i.e.,

$$dx_m = \alpha \frac{\omega_m}{\rho_0} \quad (8)$$

where  $\alpha$  is the proportionality constant.

By using the mathematical relation

$$dx_i = \frac{\partial X_i}{\partial a_m} dx_m \quad (9)$$

Cauchy's equation reduces to the form

$$\frac{\omega_i}{\rho} = \frac{1}{\alpha} dx_i \quad (10)$$

From this relation we can see that the vorticity (energy) is directly related to the length of the vortex element. When compressing a swirl in an engine cylinder, the swirl oriented in the direction of the cylinder axis is shortened but at the same time the density is increased. It can be shown, for this situation, that the vorticity is conserved.

From these considerations it was concluded that the

swirl in the engine during compression could be directly related to that in the model.

A very interesting effect was uncovered upon considering the compression of the transverse vorticity. In this case the material line element does not change (constant cylinder bore), but the density increased by compression, and thus caused the vorticity and dissipation to increase. This explains the results obtained by Lee (10), who stated that the motion (vorticity) about the cylinder axis was the only motion continuing into the expansion stroke. The transverse motion was greatly reduced in strength during compression and the viscous forces were sufficiently large to prevent this motion from continuing into the expansion stroke. Thus, from the standpoint of mixing and combustion in any engine, a swirl can best be utilized if it is uniformly oriented about the cylinder axis.

#### 4.4 Efficiency Considerations

The fin generator produced the most efficient swirl (23%). At first glance this does not seem to be a very high value, but when consideration is given to the sharp edges, torturous intake passage, turbulence in the open chamber, and the location of the reference plane, this efficiency was probably quite good.

The air swirl efficiency was calculated by considering the rotational kinetic energy of the swirl

and the reversible work spent producing the swirl. The procedure is described in detail in Appendix C. The pressure measurements for the swirl efficiency calculations were taken at a distance 9 in. from the head of the model. This was done for two reasons: (1) the swirl was nearing solid body rotation at this point and therefore the efficiency calculation was more accurate, (2) the swirl at the 9 in. location in the model corresponds approximately to TDC in the engine. The 9 in. location was chosen as the distance in the model that corresponds to one revolution in the engine (i.e., 4 in. intake stroke, 4 in. compression, and 1 in. to correct for the clearance volume).

Volumetric efficiency is the most immediate economic parameter available to compare the different swirl generation methods. Figure 4.3 shows a comparison of the static pressure loss for each of the different methods. From this information the relative volumetric efficiencies could be calculated.

<u>Method of Generation</u>	<u>Volumetric Efficiency</u>
1. None (standard engine)	81.5%
2. Fin and Shrouded Valve (72° shroud)	78%
3. Shrouded Valve (100° shroud)	74.5%
4. External Involute	71%
5. External Can	58%

These values were calculated by measuring the volumetric efficiency on the actual engine (90° shrouded valve, 76% at 1800 rpm). At the same integrated flow

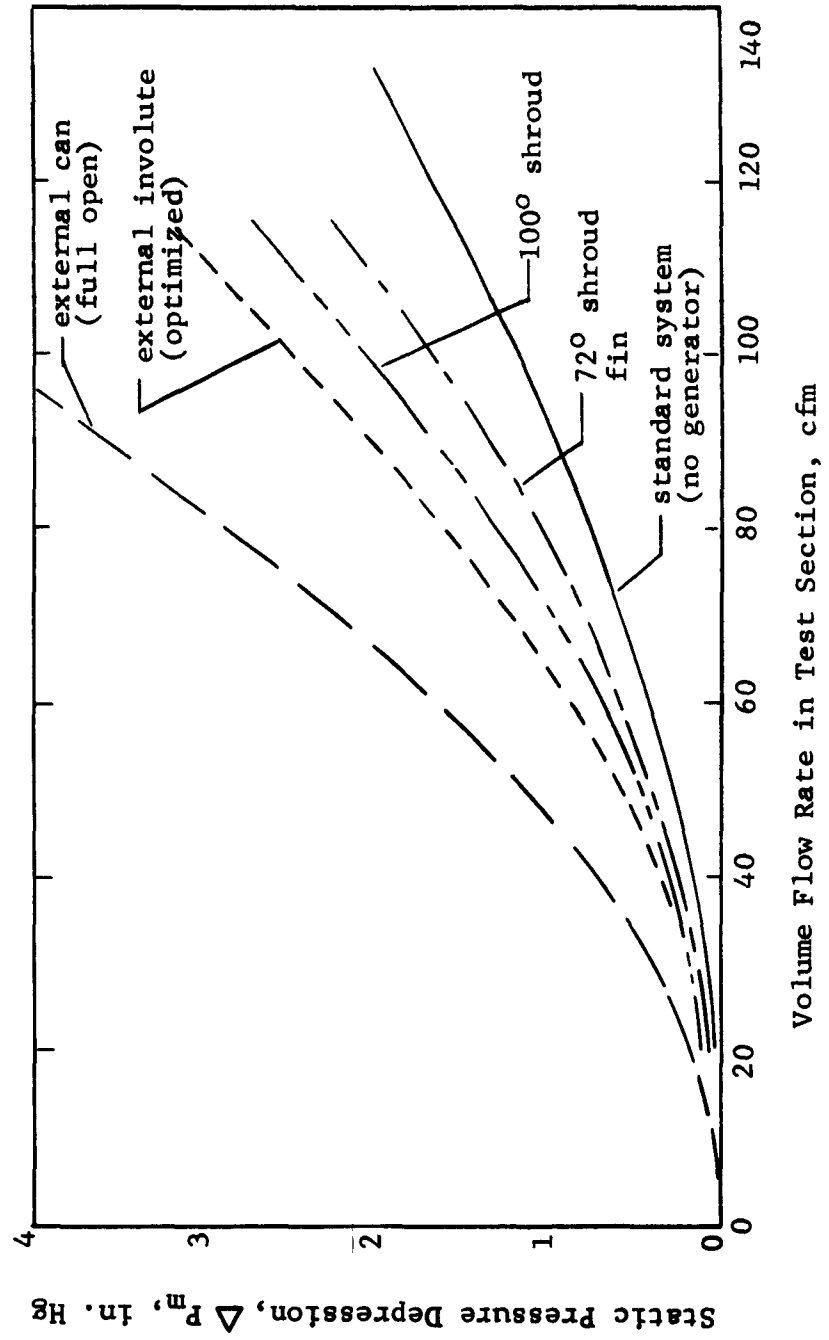


FIG. 4.3 EFFECT OF VOLUME FLOW RATE ON INTAKE PRESSURE LOSS

through the model the measured static pressure depression provided a constant relation between static pressure depression and the reduction of the volumetric efficiency from the reference. The reference was taken as 90% which was interpolated from results shown by Taylor (24) for an engine using a valve overlap of  $15^{\circ}$ .

The variable swirl generation method that is most advantageous from a cost standpoint is the fin generator. The swirl could be made variable by rotation of the fin. The device does not require an elaborate intake passage core. The fin itself could be stamped out of sheet metal. The control mechanism for this method should also be very simple.

## V. SUMMARY AND CONCLUSIONS

### 5.1 Statement of the Problem

The problem was to investigate the intake induced air swirl, and the feasibility of providing a simple method for controlling the air swirl rate for a stratified charge engine.

The investigation covered steady flow as well as turbulence and transients studies of the intake process of a four stroke cycle engine.

### 5.2 Origin and Importance of the Problem

Previous studies of the "swirl induced" stratified charge engine by Kahoun, Alperstein and Hussmann (4) used a shrouded valve for swirl generation. Some of the problems inherent in this method of swirl generation are:

- (1) The air swirl is uncontrollable (shroud angle and position are fixed)
- (2) The intake valve must be prevented from rotating (this is undesirable from the standpoint of valve life)
- (3) The volumetric efficiency of the engine is greatly reduced.

With this system good engine operation was limited to a small load range. This limited performance was due mainly to the fact that the trajectory of the injected fuel spray is a function of spray characteristics as

## V. SUMMARY AND CONCLUSIONS

### 5.1 Statement of the Problem

The problem was to investigate the intake induced air swirl, and the feasibility of providing a simple method for controlling the air swirl rate for a stratified charge engine.

The investigation covered steady flow as well as turbulence and transients studies of the intake process of a four stroke cycle engine.

### 5.2 Origin and Importance of the Problem

Previous studies of the "swirl induced" stratified charge engine by Kahoun, Alperstein and Hussmann (4) used a shrouded valve for swirl generation. Some of the problems inherent in this method of swirl generation are:

- (1) The air swirl is uncontrollable (shroud angle and position are fixed)
- (2) The intake valve must be prevented from rotating (this is undesirable from the standpoint of valve life)
- (3) The volumetric efficiency of the engine is greatly reduced.

With this system good engine operation was limited to a small load range. This limited performance was due mainly to the fact that the trajectory of the injected fuel spray is a function of spray characteristics as

well as air swirl velocity. These two factors when optimized for one operating condition are not suitable for other conditions. For good engine performance over a wide range, it is important to be able to control the air swirl rate since very little control can be exercised over the spray characteristics once the injection nozzle is selected.

### 5.3 Procedure

An air flow model was constructed to study intake induced swirl generation by different methods. The model consisted of the intake passage of a standard engine cylinder head shaped in plaster. A Rootes blower was used to draw air in through the swirl generator and model. The model was designed to simulate under steady flow conditions the intake process of an actual engine.

The air flow through the system was studied by several methods. A simple hot-wire anemometer was constructed for use in mapping the flows. Flow was also mapped with paddle wheels and visual flow observations were made with a tufted grid. Turbulence measurements were conducted with a commercial hot-wire anemometer for gaining insight into the fuel spray diffusion in the actual stratified charge engine in addition to the steady state measurements. Transient flow studies were also conducted.

A procedure was worked out for estimating the air

swirl rate in the engine and evaluated in the flow model. A method for approximating the swirl velocity in the flow model by simple static pressure measurements was worked out. This method was used to optimize the geometry of swirl generators as well as of the shrouded valve.

#### 5.4 Results and Conclusions

The results indicated that the most efficient method of generating an air swirl in an engine cylinder is with a fin type generator located inside the intake passage just ahead of the intake valve. Air swirl generation methods were compared by calculating efficiencies by the method outlined in Appendix C.

Four basic methods of swirl generation were investigated. (See Fig. 5.1) The fin generator consisted of a small piece of sheet metal which was curved and fit into the intake passage ahead of the intake valve to produce a swirl around the valve stem. The shrouded valve was a standard intake valve with a mask brazed on to block the lift area on one side and not allow air inflow on that side; swirl efficiencies were determined for two different shroud sizes. The external involute generator consisted of an involute shaped manifold external to the model head. This device generated an air swirl in the intake passage. The external can method also generated an air swirl in the intake passage by providing a tangential inlet in an enlarged section of the manifold external to

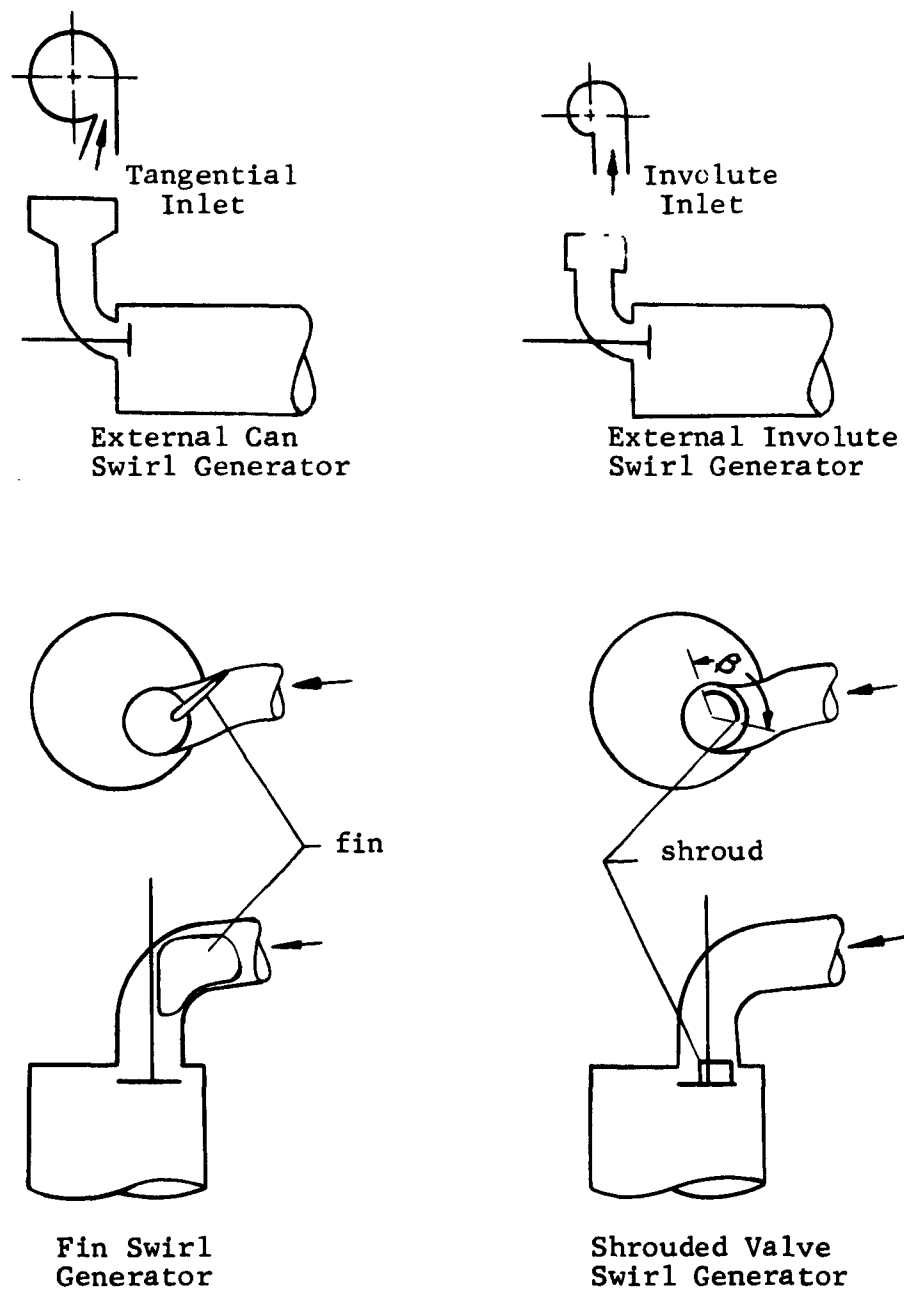


FIG. 5.1 SCHEMATICS OF SWIRL GENERATION METHODS

the model head.

<u>Method of Generation</u>	<u>Swirl Efficiency</u>
1. Fin	23%
2. Shrouded Valve (72° shroud)	21.8%
3. Shrouded Valve (100° shroud)	15.1%
4. External Involute	8.8%
5. External Can	3.9%

From these results the following conclusions may be drawn:

- (1) The fin generator was best because it generated the vortex directly along the axis of the cylinder.
- (2) The 72° shrouded valve was good for the same reason, but showed small losses from the transverse vorticity and turbulence caused by the air flowing around the bend in the intake passage.
- (3) The 100° shrouded valve was significantly poorer because of the added turbulent losses caused by the increased inflow air velocities through the unshrouded portion of the valve.
- (4) The external involute was poor because of the high viscous losses encountered in turning the vortex around the corner in the intake passage.
- (5) The external can added viscous losses by compressing and accelerating the vortex before entering the intake passage.

It was hypothesized that if an air swirl is

generated by separate means ahead (upstream) of the intake valve a more organized and stable swirl will develop, and this will result in a lower turbulence level. The test results indicated that the shrouded valve generated air swirl, which developed into a vortex like motion, had a core that spiraled along the test section. It was concluded that the spiraling of the vortex core was analogous to core precession and a nonsymmetric swirl in the engine cylinder. This motion would not be desirable from the standpoint of injected fuel trajectory. With the external swirl generator the spiraling was greatly reduced and still more so with the fin generator. The turbulence was also reduced by the latter method. This reduction of turbulence may prove to be valuable for the "swirl induced" stratification of small fuel quantities (light engine loads). While the reduction of turbulence seems desirable for part load stratification, a high level of turbulence is required for full load homogeneous operation.

### 5.5 Suggestions for Future Research

The problem of fuel distribution when a spray is injected into swirling air is a very complex problem. Presently little is known about interaction of the fuel droplets in the spray matrix and their effect on the air motion. The air motion itself contributes greatly to the fuel distribution. The air motion in the engine cylinder

is also complicated by the existence of turbulence. The following are suggested studies that would assist in understanding the "swirl induced" stratified charge system.

#### Intake Passage Design

A study of intake passage design should be conducted to include and extend the method of variable air swirl generation by the movable fin method. This should be investigated on an engine as well as a model. A study of this type should include spray injection into the air swirl for the purpose of determining the dependence of the swirl velocity on trajectory of the injected fuel spray.

#### Transient Air Swirl

Application of the flow model information should be extended to the actual engine.

An investigation of the transients in the air induction and intake induced air swirl should be conducted in a transient model or engine where air mapping and spray studies could be included. This study could include fuel sampling and stratification mapping, as well as fuel trajectory calculations using measured air flows.

#### Boundary Layer Stratification

The problem of secondary vortex stratification which occurs when an injected spray interacts with the

boundary layer is still not clearly understood. A study of injection into a steady state boundary layer would greatly simplify the complexities and help to understand the phenomena. This should also provide some insight into the problem of liquid film development and evaporation with stratification in the end boundary layer.

It is interesting to note that investigations by Kahoun, Alperstein, and Hussmann (4) indicated that the optimum injection angles were slightly upward toward the engine cylinder head. Since the engine cylinder head is the region where the secondary vortex occurs, it is important to determine the role it plays in the stratified engine operation.

#### Engine

Application of the fin system to the experimental engine would probably be the most valuable investigation. Conversion enables the effect of turbulence on ignition regularity to be studied. It would also allow performance measurements and suggest the intake passage design for this new class engine.

A more complete evaluation of the "swirl induced" stratified charge process should be conducted in an experimental engine using a quartz window in the piston for observation. With the aid of high speed photography the spray trajectory and flame development could easily be studied.

BIBLIOGRAPHY

1. J. E. Witzky, "Stratified Spark Ignition Internal Combustion Engine", United States Patent No. 2,882,873.
2. E. Fuenfer, Translation of Test Report on Fuel Injection into Rotating Air, Test Report No. XXVII, University of Munich, Germany, August 1956.
3. F. Kahoun and A. W. Hussmann, "Studies of a Stratified Charge System", The Pennsylvania State University, Technical Report, Contract Nos. DA-36-061-ORD-606 and DA-36-034-ORD-2908-RD, Department of the Army, Ordnance Corps, May 1960.
4. F. Kahoun, M. Alperstein and A. W. Hussmann, "Application of the Stratified Charge System to a Test Engine", The Pennsylvania State University, Technical Report #2, Contract No. DA-36-034-ORD-2908-RD, Department of the Army, Ordnance Corps, July 1961.
5. A. W. Hussmann, F. Kahoun and R. A. Taylor, "Charge Stratification by Fuel Injection into Swirling Air", Society of Automotive Engineers, Paper No. 598A, November 1962.
6. J. S. Meurer, "Multifuel Engine Practice", SAE Transactions, Vol. 70, pp. 712-732, 1962.
7. H. L. Wittek, "The Development of Two New Allis-Chamber Diesel Engines", SAE Transactions, Vol. 68, pp. 169-192, 1960.
8. H. R. Ricardo, "The High-Speed Combustion Engine", London and Glasgow, Blackie and Sons, 1953.
9. J. F. Alcock, "Air Swirl in Oil Engines", Proc. I.M.E., Vol. 128, pp. 123-193, 1934.
10. D. W. Lee, "A Study of Air Flow in Air Engine Cylinders", NACA Technical Report No. 653, 1939.
11. W. H. Percival, "Method of Scavenging Analysis for Two-Stroke Cycle Diesel Cylinders", SAE Transactions, Vol. 63, pp. 737-752, 1955.

12. J. A. Sobel, "Scavenging Study for Uniflow Engines", M.S. Thesis, The Pennsylvania State University, 1953.
13. R. Law and A. W. Hussmann, "Study of a Conversion of a Uniflow Two-Stroke Cycle Engine to the MAN M-system", The Pennsylvania State University, Final Report, Contract No. DA-44-009-ENG-2629, January 1958.
14. F. Pischinger, "Über Entwicklungsarbeiten an einem Verbrennungssystem für Fahrzeugdieselmotoren", Paper at Ninth International Automobile Technical Congress, London, 1962.
15. P. Schweitzer and L. J. Grunder, "Hybrid Engines", Society of Automotive Engineers, Paper No. 549A, 1962.
16. G. W. Maybach, "The Film Vaporization Combustor for Gas Turbine Engines", Engineering Research Bulletin B-75, The Pennsylvania State University, February 1959.
17. J. P. Holman and G. D. Moore, "An Experimental Study of Vortex Chamber Flow", WADC Technical Note 59-388, Wright-Patterson Air Force Base, 1959.
18. A. E. Fitzgerald and D. E. Higginbotham, "Basic Electrical Engineering", 2nd edition, New York, McGraw-Hill, 1957.
19. D. P. Margolis, "An Investigation of Curved Mixing Layers", Ph.D. Thesis, The Pennsylvania State University, 1963.
20. P. G. Hubbard, "Operating Manual for the II HR Hot-Wire and Hot-Film Anemometer, State University of Iowa, Iowa City, Iowa, Engineering Bulletin 37, 1957.
21. J. Serrin, "Mathematical Principles of Classical Fluid Mechanics", Encyclopedia of Physics, Vol. 8, Fluid Dynamics I, Springer and Verlag, Berlin, 1959.
22. Sir H. Lamb, "Hydrodynamics", Sixth edition, New York, Dover, 1932.
23. H. Schlichting, "Boundary Layer Theory", New York, McGraw-Hill, 1960.

24. C. F. Taylor, "The Internal Combustion Engine in Theory and Practice", New York, John Wiley and Sons, 1960.

APPENDIX A - HOT-WIRE ANEMOMETER TECHNIQUES

Magnitude Measurements

During the investigation a constant current hot-wire anemometer was developed and constructed to measure the mean velocity magnitude. The design of the anemometer network was based on an unbalanced Wheatstone bridge described as follows.

The voltage ( $E_a$ ) across the ammeter leg of the bridge, using the nomenclature of Fig. A, is given for the condition that  $I = 0$  by the equation

$$E_a = E \frac{R_h R_c - R R_b}{(R + R_c)(R_h + R_b)} \quad (\text{A-1})$$

This relation will be sufficient as long as the ammeter current is small compared to the total bridge current. For the ammeter then

$$E_a = I R_a \quad (\text{A-2})$$

Equation (A-1) was combined with (A-2) to get

$$I = \frac{E}{R_a} \left( \frac{R_h}{R + R_h} - \frac{R_b}{R_b + R_c} \right) \quad (\text{A-3})$$

The problem then was to pick the proper value for R

so that the bridge would have the maximum sensitivity. Since the total current through the hot wire was approximately constant the velocity was a function of wire resistance. Thus the sensitivity (S) is here defined

$$S \equiv \frac{dI}{dR_h} \quad (\text{A-4})$$

$R_a$ ,  $R_b$ ,  $R_c$ ,  $R$  and  $E$  were not functions of velocity and were held constant. Therefore

$$S = \frac{E}{R_a} \left[ \frac{R}{(R+R_h)^2} \right] \quad (\text{A-5})$$

Note that for small unbalance currents the sensitivity is not a function of balance resistors  $R_b$  and  $R_c$ .

$R/R_h$  in Equation (A-5) was replaced by  $\bar{R}$  to get

$$S = \frac{E}{R_a R_h} \cdot \frac{\bar{R}}{(1+\bar{R})^2} \quad (\text{A-6})$$

Because  $R_h$  was approximately determined by the wire material and it was important to find an order of magnitude value for  $\bar{R}$ ,  $R_h$  was held constant and  $S$  was maximized with respect to  $\bar{R}$ . This yielded

$$\bar{R} = 1.0 \quad \text{or} \quad R = R_h \quad (\text{A-7})$$

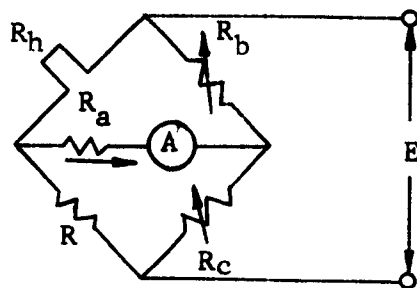


FIG. A. WHEATSTONE BRIDGE

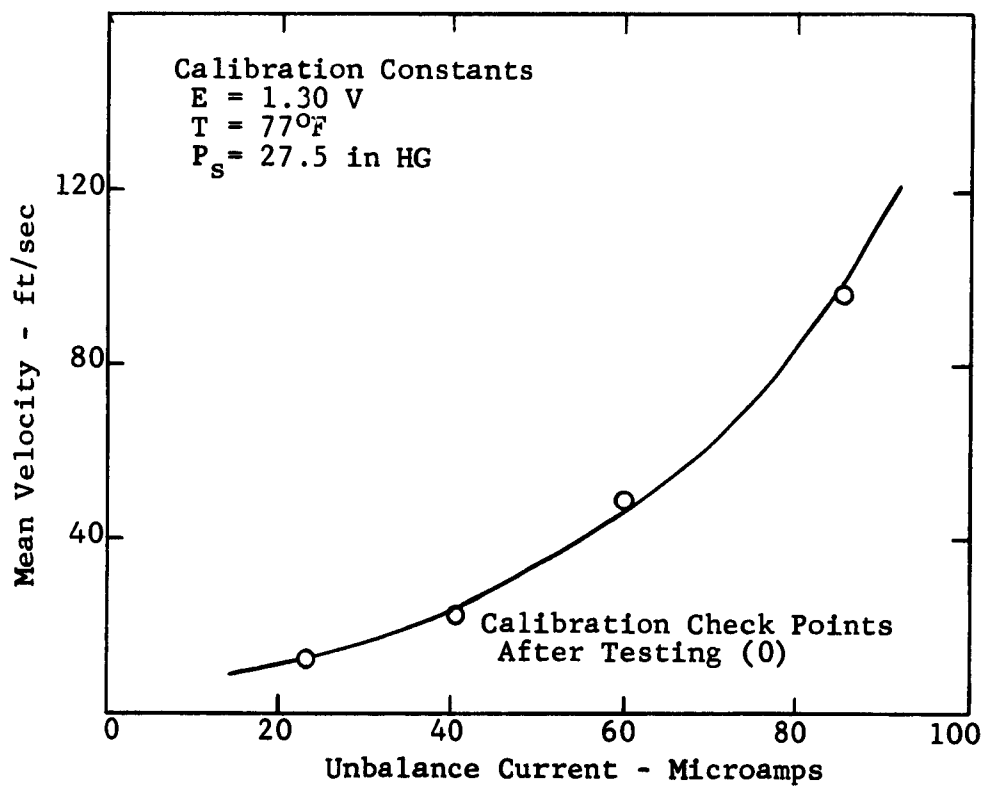


FIG. B. SAMPLE CALIBRATION CURVE FOR MAGNITUDE MEASUREMENT ANEMOMETER

Noting this a value of 1.2 ohms was found as the hot operating resistance for the size hot wire that was used (0.1 inch, 1 mil platinum). A resistor (R) was constructed from Karma alloy wire (highly insensitive to temperature) for the purpose of providing temperature independent components and reproducibility.

#### Radial Velocity Measurements

The angle ( $\psi$ ) between the calibrated flow direction and measured flow direction and the magnitude of the measured mean velocity (U) was calculated from the calibration curves by the following procedure.

The linear calibration curve was represented by the equation

$$I_c = \frac{U_c}{A} + C \quad (\text{A-8})$$

where C is the current intercept at zero velocity on the calibration curve and A is the slope of the calibration curve. (Fig. A-2) In the test section, however, the currents for both wires were equal only if the flow angle ( $\psi$ ) was zero. By considering that the heat transferred from the wire was a function of the effective length of the wire when projected normal to the flow, the actual recorded current (using the nomenclature of Fig. 2.8) were represented by the equations

$$I_1 = \frac{U}{A} \cdot \frac{\sin(\gamma_1 + \psi)}{\sin \gamma_1} \quad (\text{A-9})$$

$$I_2 = \frac{U}{A} \cdot \frac{\sin(\gamma_2 - \psi)}{\sin \gamma_2} \quad (\text{A-10})$$

where the ratio of sines is equal to the appropriate ratio of lengths.

From the calibration curve the velocities  $U_1$  and  $U_2$  were read for  $I_1$  and  $I_2$  respectively. Therefore, by equating the calibrated and measured current  $I_1$  we get

$$U \sin(\gamma_1 + \psi) = U_1 \sin \gamma_1 \quad (\text{A-11})$$

The same relation for wire 2 was found and the two equations divided by each other to eliminate  $U$  yields

$$\frac{\sin(\gamma_1 + \psi)}{\sin(\gamma_2 + \psi)} = \frac{U_1 \sin \gamma_1}{U_2 \sin \gamma_2} \quad (\text{A-12})$$

By noting the identity

$$\sin(\gamma_1 - \psi) = \cos(90^\circ - \gamma_2 + \psi)$$

and by taking  $\gamma_1 = \gamma_2 = 45^\circ$  the final relation was

$$\tan(\gamma + \psi) = \frac{U_1}{U_2} \quad (\text{A-13})$$

The flow angle ( $\gamma$ ) was found from equation (A-13). This was then replaced in equation (A-9) which was then solved for the mean flow velocity (U).

Great care was taken in constructing the probe to have  $\gamma_1$  and  $\gamma_2$  both as nearly equal to  $45^\circ$  as possible.

Figure C shows a typical calibration curve for this anemometer.

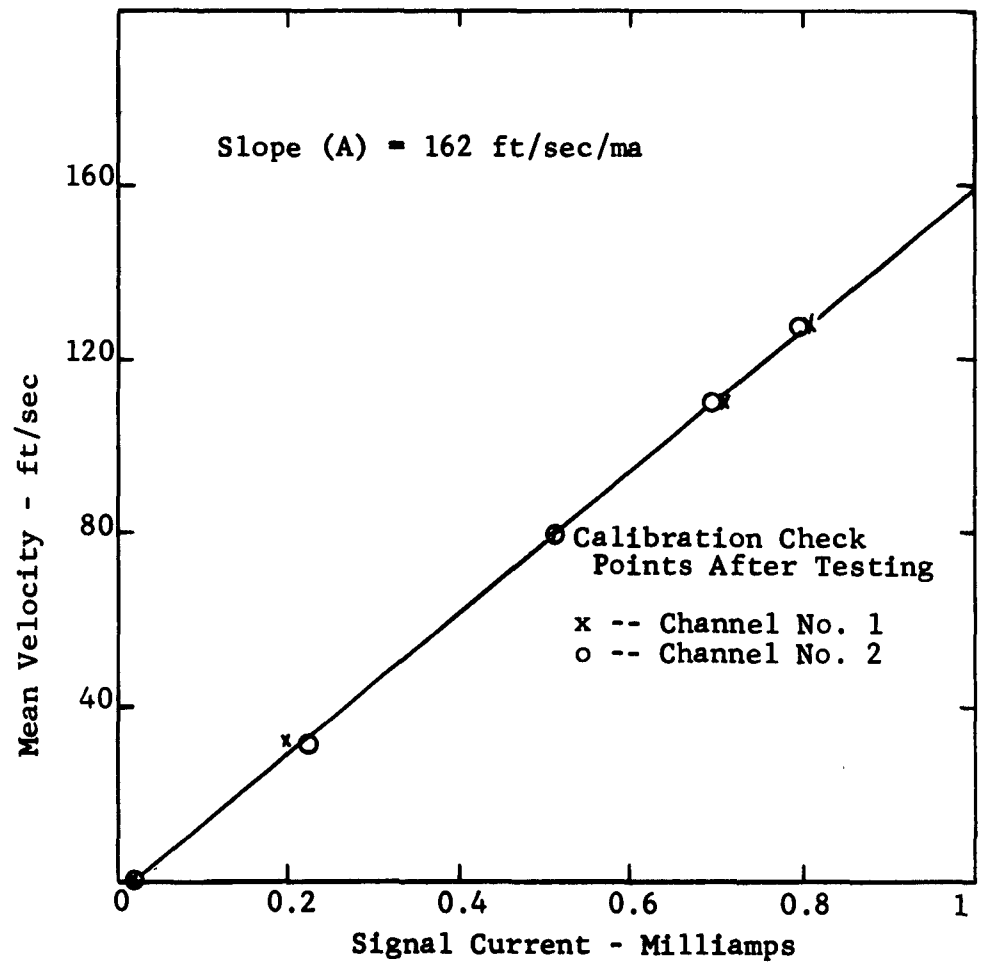


FIG. C. SAMPLE CALIBRATION CURVE FOR THE IIHR TYPE A HOT-WIRE ANEMOMETER

## APPENDIX B - SWIRL VELOCITY APPROXIMATION METHOD

There were several methods available to map the swirling air flow in the model. The approximate method discussed here was used to evaluate and optimize various test parameters prior to detailed mapping of the flow with the hot-wire anemometer. This was a very valuable method of reducing the testing time involved.

The approximate air swirl velocity in the model was determined by measuring the static core (geometrical center) and static wall pressures. This was done by placing the pressure taps in the test section sufficiently far downstream of the intake system, so that the approximation of solid body air rotation could be made. It was assumed that the flow satisfies the following restrictions:

1. The flow is nonviscous, incompressible, and subsonic.
2. The flow in the cylinder is axially symmetric and rotates with a solid body profile.

For a flow following these restrictions, the basic relationship of the static pressure gradient, radial distance, and rotational velocity component can be derived from a simple balance of the forces involved. The force acting on a fluid element owing to the static pressure gradient must be in equilibrium with the force acting on the same element due to the centrifugal action:

$$\frac{dP}{dr} = \rho \frac{V_{\theta}^2}{r} \quad \text{and} \quad V_{\theta} = r\omega_a \quad (\text{B-1})$$

where P indicates the static pressure, r the radius of curvature of the streamline,  $V_{\theta}$  the peripheral velocity component,  $\rho$  the mass density of the fluid, and  $\omega_a$  the rotational speed of the solid body air swirl about its geometric center.

With the assumptions that the fluid is incompressible ( $\rho = \text{constant}$ ) and the swirl rotates as a solid body ( $\omega_a = \text{constant}$ ) the variables can be separated and the equations integrated from the center to the chamber radius. It was necessary to use these two locations because of the difficulty involved in measuring the static pressure in a fluid moving along a curved streamline. After integrating the relation the final equation was:

$$\omega_a^2 = \frac{K h_{wc}}{\rho R^2} \quad (\text{B-2})$$

where K is the conversion constant,  $h_{wc}$  the difference between static wall and static core pressures, and R the chamber radius.

An inclined manometer was used to measure precisely the static wall to core pressure differential. The mass density was taken as that given by the static wall pressure and the free stream temperature. The absolute pressure variations were found to be less than 1%.

throughout the test section, thus the assumption of constant density was quite valid.

APPENDIX C - SWIRL GENERATION EFFICIENCY

The swirl generation efficiency ( $\eta_s$ ) was defined as

$$\eta_s \equiv \frac{KE}{W_k} \quad (C-1)$$

where KE is the rotational kinetic energy of the air swirl in the cylinder and  $W_k$  is the reversible adiabatic work corresponding to the additional pressure loss caused by the swirl generator.

For reversible adiabatic work the relation used was

$$W_k = \frac{RT_1}{1-k} \left[ \left( \frac{P_{ms}}{P_m} \right)^{\frac{k-1}{k}} - 1 \right] \quad (C-2)$$

where R is the gas constant, k is the ratio of specific heats,  $T_1$  is the initial temperature, and  $P_m$  and  $P_{ms}$  are the static pressures measured in the model for the swirl generator system and the standard intake system, respectively.

By using the assumptions of Appendix B and Equation (B-2) the rotational kinetic energy was calculated as

$$KE = - \frac{CR}{2} T_2 \frac{h_{wc}}{P_m} \quad (C-3)$$

where  $T_2$  is the temperature in the chamber,  $h_{wc}$  is the wall-to-core static pressure difference, and C is a constant to convert inches of water to inches of mercury.

The final expression was

$$\eta_s = \frac{k-1}{2} \frac{\frac{C h_{mc}}{P_m}}{\left[ \left( \frac{P_{me}}{P_m} \right)^{\frac{k-1}{k}} - 1 \right]} \quad (C-4)$$

For the calculations  $T_1$  was taken to equal  $T_2$  and  $k$  equal to 1.4.

APPENDIX D - PROCEDURE FOR ESTIMATING AIR SWIRL RATE IN THE ENGINE

Based on the assumption that the intake air flow in an engine can be simulated by steady flow, a method was worked out to approximate the air swirl in the engine. It is described here because of its contribution in understanding the investigation and its agreement with experiment.

The air flowing into the cylinder through the valve opening (opposite to the shroud) was considered as the only portion providing energy for swirl generation and the remainder provided only turbulence. If this is so, energy considerations should provide a solution for the air swirl rate.

Using the consideration that the volume flow rate is equal to the mean piston velocity and piston area, the volume flow rate (Q) through the intake valve was found from

$$Q = \eta_v \frac{\pi}{4} B^2 S \omega_e \quad (D-1)$$

where  $\eta_v$  is the volumetric efficiency, B is the cylinder bore, S is the stroke, and  $\omega_e$  is the engine speed.

The flow area ( $A_f$ ) through which the air flows was found by

$$A_f = A_e (1 - \beta/2 \pi) \quad (D-2)$$

where  $A_l$  is the lift area of the intake valve and  $\beta$  is the shroud angle. The lift area was taken at the mean valve lift position.

From the volume flow rate and the flow area the inflow velocity ( $V$ ) was calculated by

$$V = Q/A_f \quad (D-3)$$

With this the average swirl generating velocity can be found by integrating

$$\bar{V} = \int_{-\beta/2}^{\beta/2} V \cos \delta \, d\delta \quad (D-4)$$

where  $\bar{V}$  then represents the average tangential inflow velocity symmetrically across from the shroud. The fraction of the mass flow this represents is then

$\beta/(2\pi - \beta)$ . This fraction of mass was then assumed to rotate as a cylinder with a width equal to the projected width of the shroud at the radius of valve location. By considering the rotational energy of this, and by assuming that the swirl would eventually reduce to solid body rotation, kinetic energies were equated and a relation for air swirl speed ( $\omega_a$ ) was found

$$\omega_a = \frac{\bar{V}}{r_l} \sqrt{\frac{6\beta}{2\pi - \beta}} \quad (D-5)$$

where  $r_l$  is the radial location of the intake valve. By combining equation (D-1) thru (D-5) and solving the air

swirl rate (  $\omega_h/\omega_e$  ) was found

$$\omega_h/\omega_e = f(\beta, B, S \eta_v) \quad (D-6)$$

From this it was seen that the swirl rate was not a function of engine speed.